Polycyclic Bis(hydrazine) and Bis(hydrazyl) Radical Cations: High and Low Inner-Sphere Reorganization Energy Organic Intervalence Compounds

Stephen F. Nelsen,* Hao Chang, J. Jens Wolff,† and Jan Adamus‡

Contribution from the S. M. McElvain Laboratories of Organic Chemistry, Department of Chemistry, University of Wisconsin, 1101 West University Avenue, Madison, Wisconsin 53706-1396

Received March 24, 1993. Revised Manuscript Received October 13, 1993®

Abstract: Four-σ-bond-linked bis(hydrazine) radical cations **s3**$^{\bullet+}$, **a3**$^{\bullet+}$, and **a8**$^{\bullet+}$ show broad visible absorption bands with λ_{max} = 512–548 nm in CH_3CN at room temperature, attributed to Hush-type charge-transfer bands (transition energies E_{op} = 52.2–55.8 kcal/mol). The corresponding bis(hydrazyl) radical cations **s2**$^{\bullet+}$, **a2**$^{\bullet+}$, and **a7**$^{\bullet+}$ show near-IR absorption with λ_{max} = 1062–1199 nm (E_{op} = 26.9–29.3 kcal/mol). The large difference in E_{op} is caused by inner-sphere reorganization energy differences, which are predicted well by AM1 semiempirical molecular orbital calculations. Hush analysis of the absorption bands produces electronic coupling matrix elements J = 3.5 ± 0.5 kcal/mol for these species, and Marcus–Hush theory predicts intramolecular electron-transfer rate constants which are consistent with the experimental observation that ET is slow on the ESR time scale for the hydrazines and fast for the hydrazyls. The bis-*inner* hydrazyl radical cation **13**$^{\bullet+}$ exhibits a near-IR absorption band at λ_{max} = 850 nm which is narrower than those of **2**$^{\bullet+}$ and **7**$^{\bullet+}$ and is concluded not to be a Hush-type charge-transfer band.

Introduction

The free energy barrier (ΔG^*) to thermal electron transfer (ET) in Marcus theory is one-quarter of the free energy barrier for vertical ET (λ), in which the electron is transferred between the components without allowing any relaxation.[1] λ is the sum of solvent reorganization (λ_{out}) and internal geometry reorganization (λ_{in}) terms (eq 1). We shall consider only the theoretically

$$\lambda = \lambda_{out} + \lambda_{in} \quad (1)$$

simple case of "self-ET" reaction between a neutral molecule and its own radical cation, for which ΔG° = 0, and the electron-transfer rate constant k_{ex} is given by the product of a preexponential term and the exponential term containing λ (eq 2). We

$$k_{ex} = \mathrm{PRE}\ \exp(-\lambda/4RT) \quad (2)$$

have particularly studied self-ET reactions of hydrazines, which have an unusually large geometry change upon electron loss, causing a large λ_{in} value and hence unusually small k_{ex} values.[2] However, λ cannot be directly evaluated from intermolecular ET work, as several other quantities also go into determining k_{ex}. An important step in separating these quantities is measuring λ for hydrazine ET reactions, which we hoped to do by making the self-ET intramolecular instead of intermolecular.

We recently reported a practical conversion of tetracyclic bis(azo) compound **1** to the bis(*tert*-butyldiazenium) salts **2** and

Scheme I

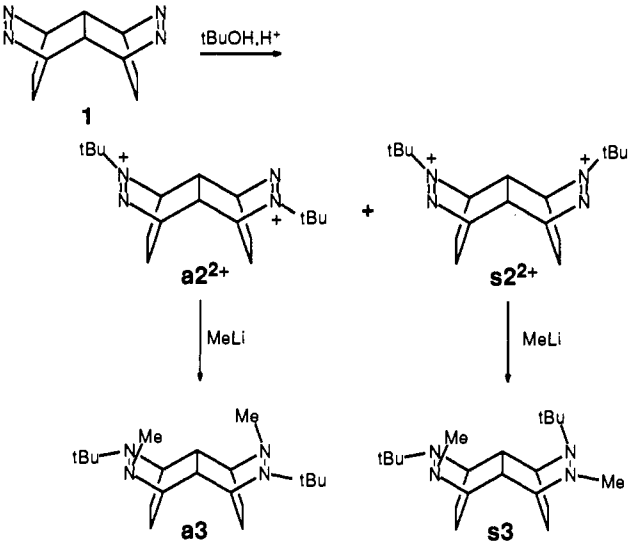

bis(*tert*-butylmethylhydrazines) **3**, as outlined in Scheme I.[3] These compounds are of interest here as precursors to radical cations which are organic analogues of the mixed-valence transition-metal complexes[4] for which Hush theory[5] has proven so successful in understanding electron-transfer properties. According to Hush theory, a charge-transfer (CT) optical absorption corresponding to vertical electron transfer (ET) between the redox centers will be observed if electronic interaction at the transition state is large enough. The transition energy for the charge-transfer band, E_{op}, is the energy gap between the ground state, which has both redox centers and their solvation shells relaxed, and the CT state with an electron transferred but no relaxation. E_{op} is an experimental measure of the Marcus λ value.[1]

† Present address: Organisch-Chemisches Institut der Universität Heidelberg, Im Neuenheimer Feld 270, D-6900 Heidelberg, FRG.

‡ Present address: Institute of Applied Radiation Chemistry, Technical University (Politechnika) Łódź, Wróblewskiego 15, Poland.

* Abstract published in *Advance ACS Abstracts*, December 1, 1993.

(1) For recent reviews of electron-transfer theory, see: (a) Sutin, N. *Prog. Inorg. Chem.* **1983**, *30*, 441. (b) Marcus, R. A.; Sutin, N. *Biochim. Biophys. Acta.* **1985**, *811*, 265.

(2) For reviews of hydrazine electron-transfer work, see (a) Nelsen, S. F. *Acc. Chem. Res.* **1981**, *14*, 131. (b) Nelsen, S. F. In *Molecular Structures and Energetics*; Liebman, J. F., Greenberg, A., Eds.; VCH Publishers, Inc.: Deerfield Beach, FL, 1986; Vol. 3,Chapter 1, pp 1–86. (c) Nelsen, S. F. In *Advances in Electron Transfer Chemistry, Vol. 3*, Mariano, P. S., Ed.: JAI: Greeenwich, CT, in press.

(3) Nelsen, S. F.; Wolff, J. J.; Chang, H. *J. Am. Chem. Soc.* **1991**, *113*, 7882.

(4) For a review, see: Creutz, C. *Prog. Inorg. Chem.* **1983**, *30*, 1.

(5) (a) Hush, N. S. *Trans. Faraday Soc.* **1961**, 57, 557. (b) Allen, G. C.; Hush, N. S. *Prog. Inorg. Chem.* **1967**, *8*, 357; 391. (c) Hush, N. S. *Coord. Chem. Rev.* **1985**, *64*, 135. (d) Hush, N. S. In *Mixed Valence Compounds*; Brown, D. B., Ed., Reidel: Dordrecht, the Netherlands, 1980; p 151.

0002-7863/93/1515-12276$04.00/0

In this work we hoped to measure λ using the Hush method for intramolecular ET in bis(hydrazine) radical cations, shown as $A^{\bullet+}$ below. Comparison of $A^{\bullet+}$ with bis(hydrazyl) radical

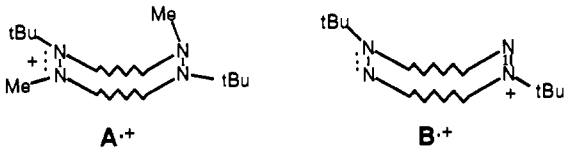

cations $B^{\bullet+}$ was also an important goal of this work. The spin-bearing dinitrogen units of $A^{\bullet+}$ [2] and $B^{\bullet+}$ [6] are similar, with the odd electron in a π^*(NN) orbital. Their diamagnetic dinitrogen units are very different, the hydrazine unit of $A^{\bullet+}$ having pyramidal nitrogens and a long N–N single bond length and the diazenium cation unit of $B^{\bullet+}$ a planar *tert*-butylated nitrogen and a short N–N double bond length. Clearly, smaller geometry change upon vertical ET occurs for $B^{\bullet+}$ than for $A^{\bullet+}$. The geometry change in $B^{\bullet+}$ ET ought to be more like the second (radical cation, dication) ET of hydrazines than the first ET, and λ_{in} should be smaller for $B^{\bullet+}$. We showed in an intermolecular case that the second ET for a sesquibicyclic hydrazine is faster than the first despite the work term necessary for approach of a dication to a cation.[7] We hoped to establish whether the prediction of very different optical properties for $A^{\bullet+}$ and $B^{\bullet+}$ is true and to examine the application of Hush theory to these organic radical cations, which we expected to differ from mixed-valence transition-metal compounds by having much larger E_{op} values (for $A^{\bullet+}$) and higher frequency vibrational couplings. We previously investigated the oxidation of several bis(hydrazines),[8] but the connecting links between the nitrogens in the compounds studied were too flexible to define the radical cation geometry very well, and these studies were plagued by short radical cation lifetimes. The rigidity of the double, four-σ-bond linkages of $2^{\bullet+}$ and $3^{\bullet+}$ were expected to provide relatively long lifetimes. Here we study 2^{2+} and **3** and some analogues prepared from other bis(azo) compounds, comparing their ET thermodynamics measured by cyclic voltammetry and the spectral properties of their radical cation oxidation states with Marcus–Hush theory.

Compound Preparation

As discussed previously,[3] we prepared **1** by Shen's route,[9] hydrogenating diene **4** (the basketene, bis(diethylazodicarboxylate) adduct, see Scheme II) before hydrolysis and oxidation. We also repeated Shen's 2 + 2 photoclosure prior to azo compound formation, producing his hexacyclic bis(azo) compound **6**, and converted **6** to the hexacyclic diazenium salts 7^{2+} and hydrazines **8** as outlined in Scheme II. Separation of the diazenium salts 7^{2+} by crystallization proved more difficult than for the 2^{2+} salts.[3] Although **a**7^{2+} free from the *syn* isomer by ^{13}C NMR was obtained by multiple crystallizations, our sample of **s**7^{2+} contained about 15% of the *anti* isomer. Methylation of **a**7^{2+} produces hexacyclic hydrazine **a8**, which in $CDCl_3$ is a mixture of two symmetrical conformations (eight carbons each by ^{13}C) and a minor, unsymmetrical one (two *t*Bu CCH_3 by ^{13}C NMR, several of the

Scheme II

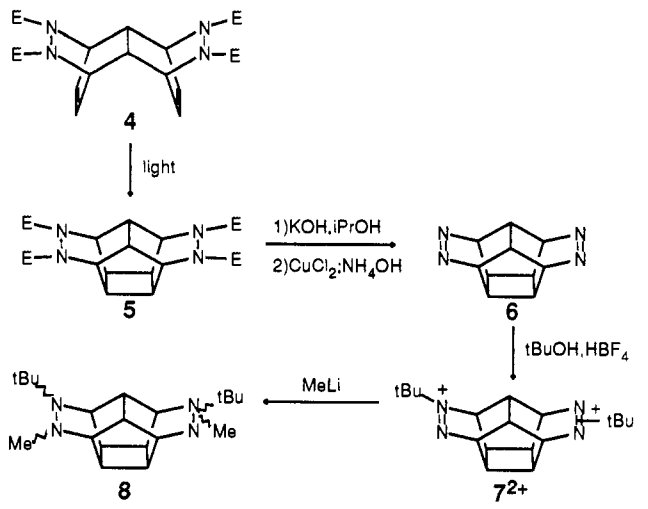

less intense of the 14 other carbons which must be present not clearly observed). Only *trans*-dialkylated hydrazine units are

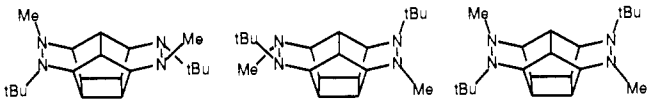

a8: **Oi,Oi** **Io,Io** **Oi,Io**

reasonable conformations for **a8**.[3] The unsymmetrical conformation can only be **Oi,Io** (and its enantiomer **Io,Oi**), while the symmetrical ones are the bis-*tert*-butyl "Out" and "In" conformations **OiOi** and **IoIo**. Integrations of the ^{1}H NMR NCH_3 and CCH_3 signals were consistent with mole fractions 0.56_5:0.29_0:$0.14_5 \pm 0.005$, making their relative free energies 0.0, 0.4, and 1.2 kcal/mol. These conformational isomers of **a8** are much closer in energy than are those of **a3**, where only **OiOi** is detectably occupied by NMR,[3] doubtless because ring torsion is less in the hexacyclic **a8** than in the tetracyclic **a3**. MM2 molecular mechanics calculations[10] for these conformations give the following relative strain energies: for **a3**, **Oi,Oi** 0.0, **Io,Io** 1.6, and **Io,Oi** 4.3 kcal/mol; and for **a8**, **Oi,Oi** 0.0, **Io,Io** 0.4, and **Io,Oi** 1.8 kcal/mol, in apparent excellent agreement with experiment.[11] We failed to separate pure enough **s8** from the methylation product of the 85% **s**7^{2+} mixture for meaningful spectral measurements.

2^{2+}/**3** and 7^{2+}/**8** share the dinitrogen units being substituted *outer* on the bicyclo[2.2.2]octane units fused at the central C–C bond. We used Prinzbach's proceedure to convert Vogel's methano-bridged cyclodecapentene[12] **9** to the bis(*inner* azo) compound **12**,[13] which was *tert*-butylated to the *anti* bis(diazenium) salt 13^{2+} (see Scheme III). We did not observe NMR peaks attributable to either *syn* isomer of 13^{2+}, and we

(6) (a) Nelsen, S. F.; Landis, R. T., II. *J. Am. Chem. Soc.* **1973**, *95*, 2719. (b) Nelsen, S. F.; Landis, R. T., II. *J. Am. Chem. Soc.* **1974**, *96*, 1788. (c) Use of tetamethylammonium thiophenylate as the reductant for 21^+ results in formation of a weak purple color caused by a species with λ_m of 520 nm, which is apparently not a radical because the ESR spectra are similar for the purplish solutions generated by thiophenylate reduction and the yellowish ones generated by electrolytic reduction. It seems possible that this color is caused by charge transfer from residual PhS$^-$ 21^+ pairs, but this point has not been investigated here.

(7) Nelsen, S. F.; Blackstock, S. C.; Kim, Y. *J. Am. Chem. Soc.* **1987**, *109*, 677.

(8) Nelsen, S. F.; Willi, M. R.; Mellor, J. M.; Smith, N. M. *J. Org. Chem.* **1986**, *51*, 2081.

(9) (a) Shen, K. W. *J. Chem. Soc., Chem. Commun.* **1971**, 391. (b) Shen, K. W. *J. Am. Chem. Soc.* **1971**, *93*, 3064.

(10) (a) MM2 calculations: Allinger, N. L. *J. Am. Chem. Soc.* **1977**, *99*, 8127. Allinger, N. L.; Yuh, Y. *QCPE Bull.* **1980**, *12*, 395. (b) The sucess of MM2 calculations on predicting relative energies of conformations of these compounds is a result of their special conformational constraints; see: Nelsen, S. F.; Wang, Y.; Powell, D. R.; Hayashi, R. K. manuscript submitted for publication.

(11) (a) Unfortunately, the lack of resolution of the central bond and four-membered-ring C*H* signals, even at 500 MHz, precludes confident use of NOSEY experiments, which were used to prove that **a3** is in the **Oi,Oi** conformation,[3] to experimentally verify the identification of A with **Oi,Oi**. The chemical shift difference between the four-membered-ring *CH* signals is very different for the two isomers (δ 0.08 for A and δ 4.6 for B), while that between the CH_2 signals of **a3** is δ 5.6 , which would seem more consistent with B being **Oi,Oi** than with A, but it does not prove it. (b) CCCC twist angles at the central bond: (**a3**) **Oi,Oi** 11.9°, **Io,Io** 9.0°, **Io,Oi** 3.5 and 9.5°; (**a8**) **Oi,Oi** 4.9°, **Io,Io** 4.9°, **Io,Oi** 1.1 and −0.9°.

(12) Vogel, E.; Klug, W.; Breuer, A. *Org. Synth.* **1974**, *54*, 11.

(13) Prinzbach, H.; Fischer, G.; Rihs, G.; Sedelmeier, G.; Heilbronner, E.; Yang, Z. Z. *Tetrahedron Lett.* **1982**, *23*, 1251.

(14) Ammar, F.; Savéant, J. M. *J. Electroanal. Chem. Interfacial Electrochem.* **1973**, *47*, 115; 215.

Scheme III

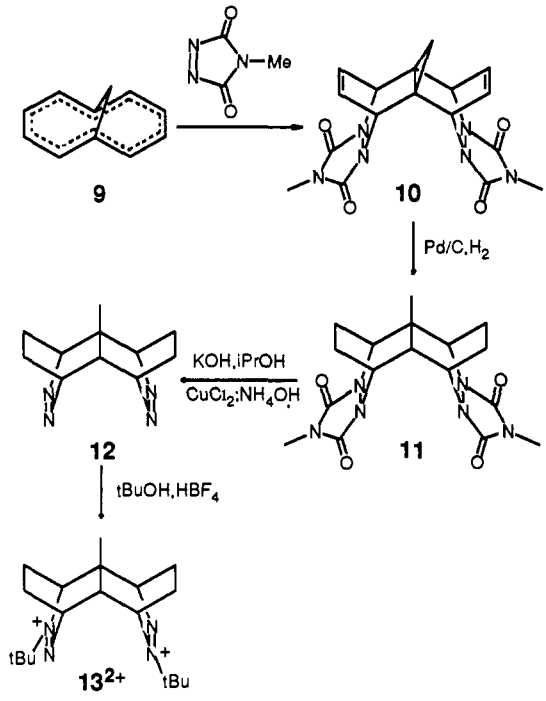

were unsuccessful in attempts to isolate a hydrazine from the reaction of 13^{2+} with methyllithium.

Results and Discussion

Cyclic Voltammetry. The thermodynamics for electron removal from **A** and **B** were studied by cyclic voltammetric determination of their formal redox potentials, $E°$. Although the hydrazines were scanned through two oxidations followed by two reductions and the diazenium salts through two reductions followed by two oxidations, it is most convenient to compare them starting from the neutral forms. The electron transfers are all chemically reversible, exhibiting equal oxidation and reduction currents for both waves. They are electrochemically quasireversible, the hydrazines exhibiting 60–80 mV peak-to-peak separations (ΔE_{pp}) and the diazenium salts 60–85-mV separations in acetonitrile at slow scan rates. The $E°$ values reported are $(E_p^{ox} + E_p^{red})/2$ for cases exhibiting well-separated waves and were determined by comparing the experimental curves with simulations of overlapping quasireversible waves when $\Delta E°$ was under 0.2 V. The CV data in acetonitrile are summarized in Table I, and data in dimethyl sulfoxide (for **B**) and methylene chloride (for **A**) are discussed in the supplementary material.

A compound with two equivalent, noninteracting redox sites shows a cyclic voltammogram having a single wave of the same ΔE_{pp} and shape but twice the current as that for a compound with only one redox site at the same concentration. The observed wave is caused by the overlap of two one-electron waves having a statistically determined $\Delta E° = E_2° - E_1°$ of 35.6 mV at 25 °C.[15,16] We therefore tabulate values of $\Delta E_1°$ (eq 3) in Table

$$\Delta E_1°, \text{V} = E_1° - E°(\text{mono}) + 0.018 \qquad (3)$$

I to allow proper comparison of the ease of removal of the first electron from the bis systems with that for the "monomeric" single redox site compounds, hydrazine **14** and hydrazyl $\mathbf{15}^{\bullet 0}$. The $\Delta E_1°$ values are small and negative for the tetracyclic hydrazines **s3** and **a3**, but the hexacyclic hydrazine **a8** is 1.4 kcal/mol harder to oxidize than **14**, possibly because the hexacyclic framework

(15) Flanagan, J. B.; Mangel, S.; Bard, A. J.; Anson, F. C. *J. Am. Chem. Soc.* **1978**, *100*, 4248.
(16) Rehm, D.; Weller, A. *Z. Phys. Chem., N. E.* **1970**, *69*, 183.

Table I. Cyclic Voltammetry Data in Acetonitrile

compd	$E_1°, E_2°$ [a] (V)	$\Delta E_1°$ [b] (kcal/mol)	$\Delta E°'$ [c] (kcal/mol)	N–N distance[d] (Å), AM1[X-ray]
	Hydrazines			
14 ("mon")	+0.10, –	≡0		
s3 (tet)	+0.06, +0.21	–0.5	+2.6	4.89 [4.85]/4.91
a3 (tet)	+0.04, +0.18	–0.9	+2.6	4.88 [4.81]/4.87
a8 (hex)	+0.14, +0.36	+1.4	+4.3	5.01/4.98
	Hydrazyls			
15 ("mon")	-0.79_5, –	≡0		
16	-0.64_5, –	+3.5		
s2 (tet)	-0.74_5, –0.40	+1.6	+7.1	4.85/4.83
a2 (tet)	-0.75_5, –0.41	+1.4	+7.1	4.85 [4.74]/4.84
s7 (hex)[e]	-0.76_5, –0.37	+1.2	+8.3	4.95/4.94
a7 (hex)	–0.77, -0.39_5	+1.0	+8.2	4.95/4.95
13 (tet *inner*)	–0.76, –0.04	+1.3	+15.8	2.92/2.84

[a] In acetonitrile containing 0.1 M n-Bu_4NClO_4, Pt electrode, room temperature, vs a saturated calomel electrode. [b] Difference in $E_1°$ from "monomeric" compound, corrected for statistical effect using eq 3 of the text. [c] Difference in $E°$ values for second and first electron removal, corrected for statistical effect using eq 4 of text. [d] Average of closest N–N distances in neutral hydrazines and diazenium dications; after slash, in the radical cations. [e] 15% **a7** in sample.

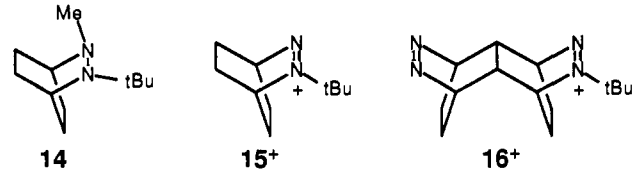

restricts torsion. $\Delta E_1°$ values are all positive for the bis(hydrazyls) and similar in size for the tetracyclic and hexacyclic compounds. A smaller $\Delta E°'$ range seems reasonable because the hydrazyl/diazenium cation electron loss causes less of a geometry change than the hydrazine/hydrazine radical cation oxidation, so differences in flexibility of the polycyclic compounds should be less important. The neutral tetracyclic and hexacyclic bis(hydrazyls) differ from $\mathbf{15}^{\bullet 0}$ by having hydrazyl nitrogens four σ bonds away from the hydrazyl being oxidized. That detectable effects can be transmitted through four σ bonds is indicated by the 3.5 kcal/mol more positive $E°$ value for the azo-substituted monohydrazyl derived by reduction of $\mathbf{16}^{+}$ than for $\mathbf{15}^{\bullet 0}$. The more planar hydrazyl nitrogens may be more electron-withdrawing than hydrazine nitrogens and also contribute to the observed more positive $\Delta E_1°$ values for bis(hydrazyls) than for bis(hydrazines). The differences between the two oxidation potentials, corrected for the statistical effect, which we will call $\Delta E°'$ (see eq 4), are

$$\Delta E°', \text{kcal/mol} = 23.06(E_2° - E_1° - 0.036) \qquad (4)$$

also given in Table I. $\Delta E°'$ ought to be affected by electrostatics (removal of the second electron requires a "through space" electrostatic *w*ork term, $\Delta E_w°$, because the oxidized dinitrogen unit bears a positive charge), "*t*hrough *b*ond" effects ($\Delta E_{tb}°$; the charges in the dication will also interact through the σ-bonds connecting the dinitrogen units), and *ion*pairing/solvation effects, $\Delta E_{ip}°$ (see eq 5).

$$\Delta E°' = \Delta E_w° + \Delta E_{tb}° + \Delta E_{ip}° \qquad (5)$$

The distances between the dinitrogen units of these compounds are constrained by the polycyclic connecting units, and the N–N′ distances **d** estimated by AM1 semiempirical molecular orbital calculations are compared with X-ray geometric data for the three available cases in the last column of Table I. The AM1 distances are slightly larger than the X-ray distances, but the differences are rather small, and the relative sizes of the **d** values should be reliable. The dinitrogen units are held nearly parallel to each other, and it makes no significant difference in estimating

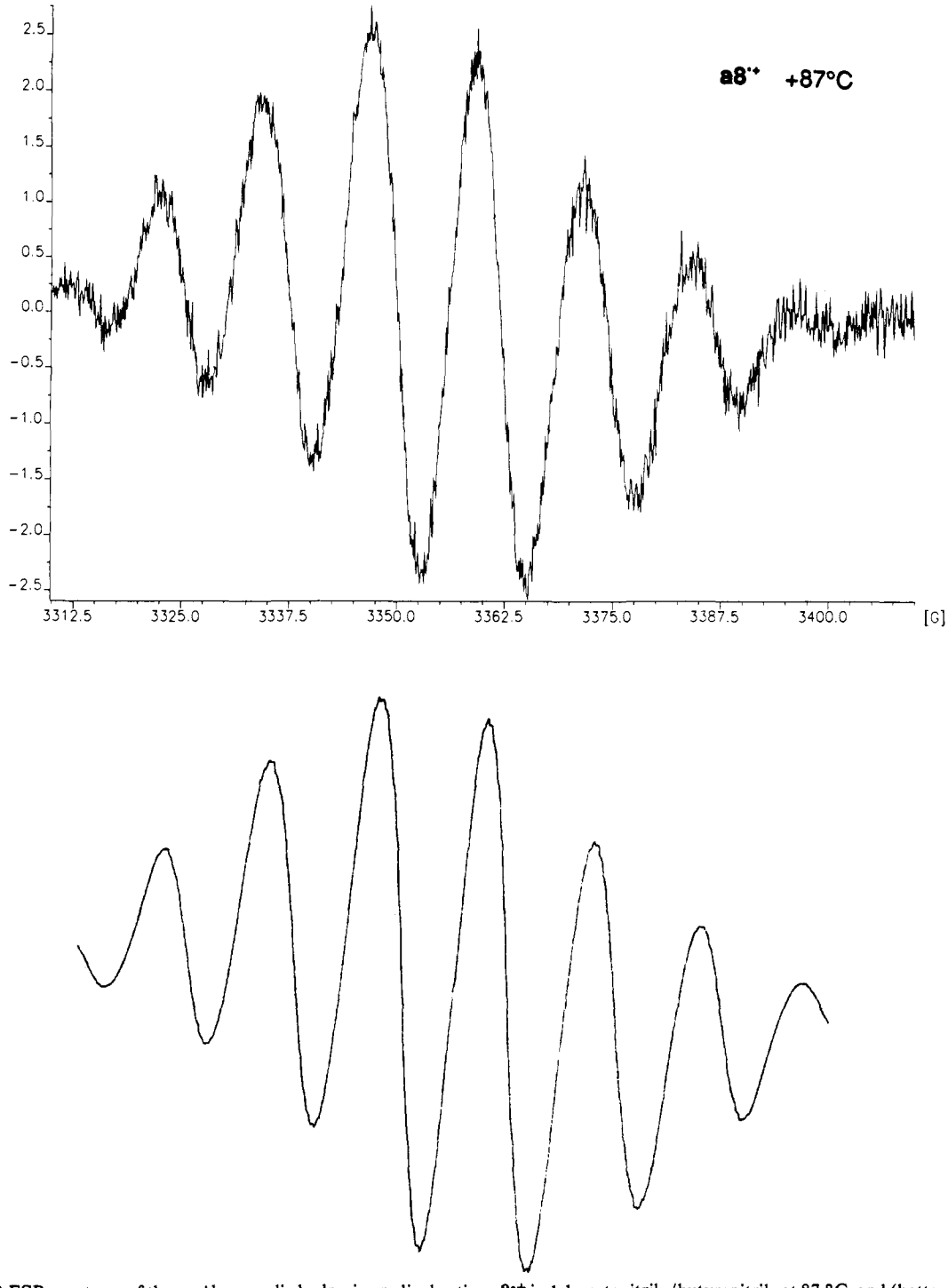

Figure 1. (Top) ESR spectrum of the *anti* hexacyclic hydrazine radical cation **a8**$^{\bullet+}$ in 1:1 acetonitrile/butyronitrile at 87 °C, and (bottom) a simulation for a slow exchange spectrum (see text).

the work term whether full charges at the average dinitrogen distance quoted or contributions of charges of $^1/_2$ at each nitrogen are summed. We use the averaged AM1 d values in this work. The electrostatic work term for two point charges separated at a distance d (Å) in a medium of dielectric constant ϵ is given by eq 6. It has been traditional to use the solvent dielectric constant

$$W = e^2/d\epsilon = 332.1/d\epsilon \qquad (6)$$

ϵ_s and the distance between centers when the molecules touch in the work term for electron-transfer considerations, as for example in the Rehm–Weller equation[16] and in Marcus theory.[1] The ϵ_s(25 °C) value for CH_3CN is 35.94 D. As Suppan has pointed out for CT ion pairs,[17] it seems unrealistic to expect that an intermolecular electrostatic work term would be as small as that obtained using the bulk solvent ϵ_s, because if the molecules touch, there is no solvent between them. Suppan suggests employing the much larger number obtained by using a hydrocarbon ϵ_s value, about 2 D, as the effective dielectric constant, ϵ_{eff}, for use in eq 6 to estimate the work term. This appears unrealistic to us because solvent is present to mediate the interaction between the charges, although not directly between the charged units. The large $\Delta E^{\circ\prime}$ for **13** is presumably principally caused by the close proximity of the *inner* diazenium cation units in the dication, which is only consistent with an ϵ_{eff} value significantly lower than that for bulk acetonitrile. Because the connecting σ bonds are not in the favorable *anti* arrangement for strongest through bond inter-

(17) Suppan, P. *J. Chem. Soc., Faraday Trans. 1* **1986**, *82*, 509.

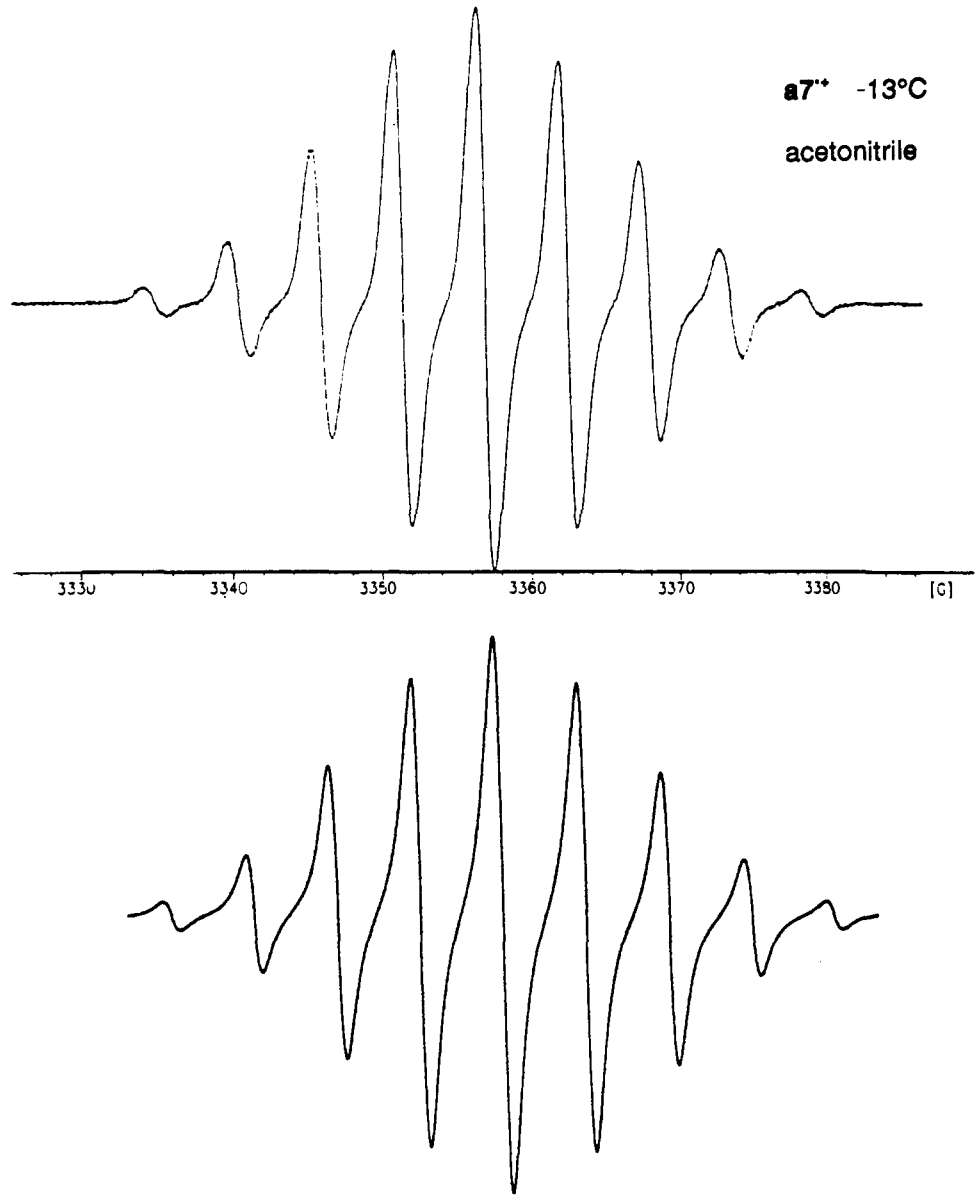

Figure 2. (Top) ESR spectrum of the *anti* hexacyclic hydrazyl radical cation **a7**$^{\bullet+}$ in acetonitrile at −13 °C, with (bottom) a simulation for fast exchange [a(4N) = 5.5 G, line width 1.0 G].

action,[5c] the contribution of $\Delta E_{tb}°$ to $\Delta E°'$ cannot reasonably be larger than that for **a2**$^{\bullet+}$, and the minimum $\Delta E_w°$ contribution ought to be ca. 11.3 kcal/mol. The minimum effective distance between the dinitrogen units reasonable to use is the 2.84-Å value of d, so use of eq 6 to estimate the effective ϵ value in acetonitrile produces $\epsilon_{eff} \leq 10.3$ D, or <29% of the ϵ_s of acetonitrile.

ESR Studies. Results. The "monomeric" hydrazine radical cation **14**$^{\bullet+}$ was generated by $NOPF_6$ oxidation in acetonitrile. Its ESR spectrum is complex, but the large splittings by two different nitrogens and a methyl group produce a pattern of eight overlapping multiplets of lines with an average separation of about 12 G. The spectrum at −40 °C was approximately fit by a simulation employing a(N) = 14.3, a(N′) = 13.2, and a(3H) = 10.5 G, as well as a smaller splitting of a(4H) of 2.1_5 G (which represents an average of the two different *exo* CH_2 spittings present), and a line width of 1.2 G. Study of analogous compounds shows that the *endo* CH_2 splitting should be smaller (it is 0.6 G for the 2,3-dimethyl-2,3-diazabicyclo[2.2.2]octane radical cation[6a]) and the bridgehead splitting far too small to resolve.

Oxidation of **3** and **8** produces purplish solutions which, as expected from previous work on bis(hydrazine) radical cations,[8] have ESR spectra for which ET is slow on the ESR time scale. Both **s3**$^{\bullet+}$ and **a8**$^{\bullet+}$ give spectra having eight complex multiplets with about 12-G peak separation. Heating a sample of **a8**$^{\bullet+}$ in 1:1 acetonitrile:butyronitrile to 87 °C resulted in loss of the complex fine structure observed at −23 °C, but did not change the relative intensities of the large splitting pattern. The spectrum resembles that simulated for splittings of 13.9 (1N), 13.2 (1N), and 10.6 (3H) G, with a large line width simulated by a 2-G Lorentzian line width plus added smaller splittings (see Figure 1). Although some line broadening occurs as the temperature is raised, there is no evidence from relative peak intensities that the broadening arises from intermolecular ET, and the intramolecular ET rate constant is concluded to be small on the ESR time scale.

"Monomeric" hydrazyl radical **15**$^{\bullet 0}$ gives similar ESR spectra when prepared by electrochemical reduction[6] and by treatment with tetramethylammonium thiophenoxide ($Me_4N^+PhS^-$), which proved to be a convenient reagent for this purpose. The room temperature ESR spectrum of **15**$^{\bullet 0}$ consists of five groups of badly overlapping signals, which were reasonably simulated using splittings of 11.00 (1N) and 10.6_2 (1N) G, with ill-determined small splittings of 2.8_2 (2H), 1.8_2 (2H), 0.8_6 (2H), and 0.5_7 (2H) G, and a line width of 1.4 G.

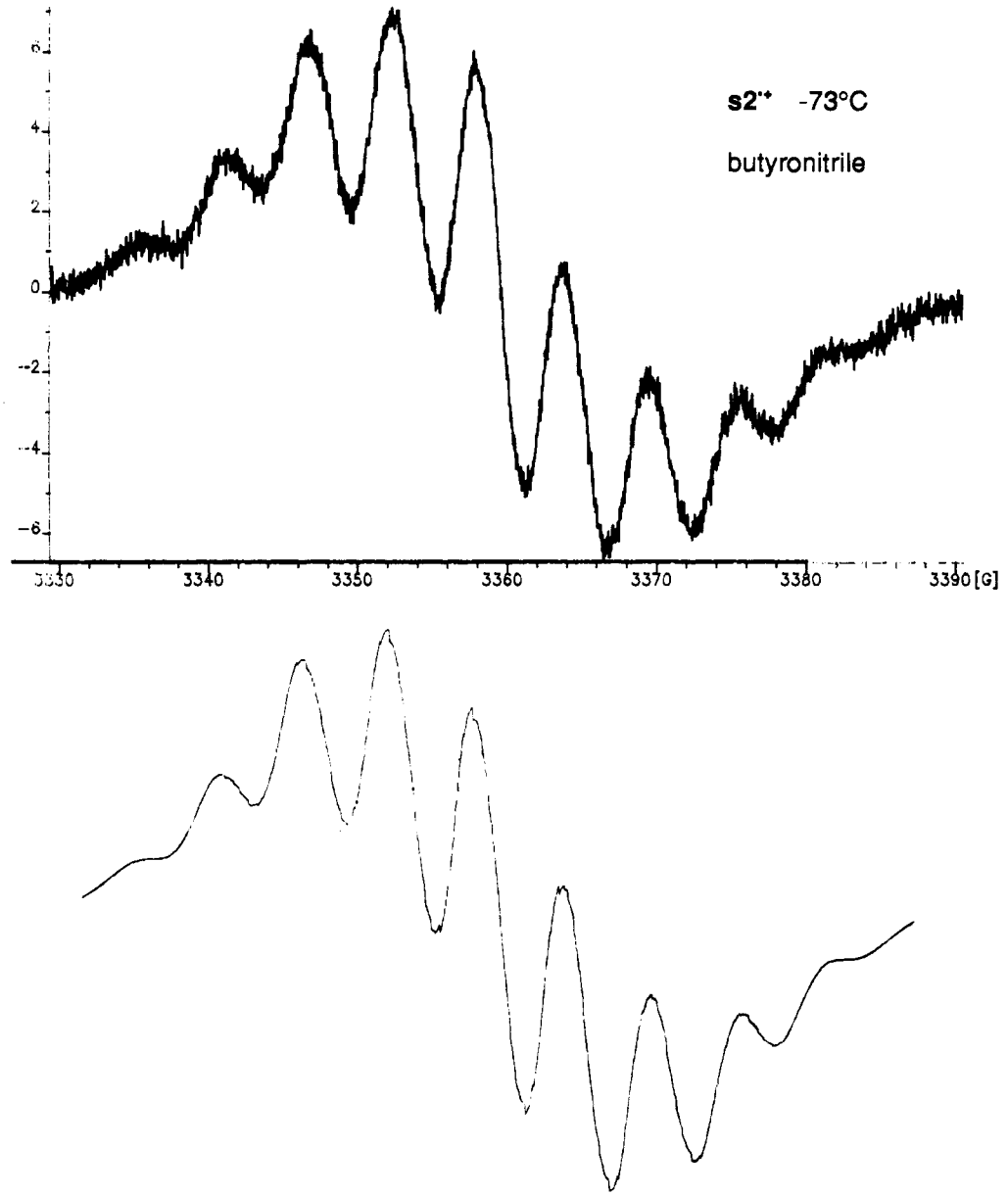

Figure 3. (Top) ESR spectrum of the *syn* tetracyclic hydrazyl radical cation $\mathbf{s2}^{\bullet+}$ in butyronitrile at −73 °C, with (bottom) a simulation for fast exchange [a(4N) = 5.5 G and a large line width, see text].

Reduction of $\mathbf{2}^{2+}$ and $\mathbf{7}^{2+}$ isomers gives blue-green solutions. $\mathbf{a7}^{\bullet+}$, which lacks any large a(H) *exo* hydrogens, shows a simple nine-line ESR pattern at −13 °C which is well simulated using a(4N) = 5.5 G with a line width of 1.0 G (see Figure 2). ET between the dinitrogen units is fast on the ESR time scale, and neither the difference between the di- and trisubstituted nitrogens nor any hydrogen hyperfine splitting has been resolved. The spectrum of $\mathbf{s2}^{\bullet+}$ also shows a nine-major line pattern, but the lines are much broader, and there are ill-resolved splittings in the range of 1.5–1.8 G in the outer lines at room temperature. Cooling $\mathbf{s2}^{\bullet+}$ generated by phenylthiolate reduction in butyronitrile slightly increases broadening, and the smaller splittings are no longer evident. The ESR spectrum at −73 °C is reasonably well fit by a simulation using a(4N) = 5.5 G, with a broad line width introduced by including splitting of 1.7 (4H) and 0.6 (4H) G along with a line width of 1.7 G (see Figure 3) . At still lower temperatures, the outer lines broaden greatly, presumably caused by the nonuniform line width effects induced by slow tumbling when spin 1 atoms bearing significant spin are bonded, which cause the $M_N \neq 0$ lines of several hydrazine radical cations to disappear entirely at low temperature.[18] We have not observed the line alternation expected for ET between the two dinitrogen units becoming slow on the ESR time scale at any temperature. We conclude that even at −73 °C, $\mathbf{s2}^{\bullet+}$ shows rapid intramolecular ET.

Reduction of $\mathbf{13}^{2+}$ gives a blue-green solution having an ESR spectrum showing many ill-resolved lines, which we have not been able to interpret (the four different N and five different *exo* splittings in principle lead to 2592 lines). The g-factor and total width are similar to those of the spectra from $\mathbf{2}^{2+}$ and $\mathbf{7}^{2+}$, and we assign this species as $\mathbf{13}^{\bullet+}$.

ESR Studies. Discussion. The most important result of the ESR studies is that the four-σ-bond-linked examples of $\mathbf{B}^{\bullet+}$ show much faster intramolecular ET than the corresponding $\mathbf{A}^{\bullet+}$ compounds, which is consistent with the large difference in λ_{in} expected. These ESR studies demonstrate that long-lived hydrazine radical cations and hydrazyls are generated and allow limits to be placed on intramolecular ET rate constants. Intramolecular electron exchange in $\mathbf{B}^{\bullet+}$ interconverts a pair of

(18) Nelsen, S. F.; Weisman, G. R.; Hintz, P. J.; Olp, D.; Fahey, M. R. *J. Am. Chem. Soc.* **1974**, *96*, 2916.

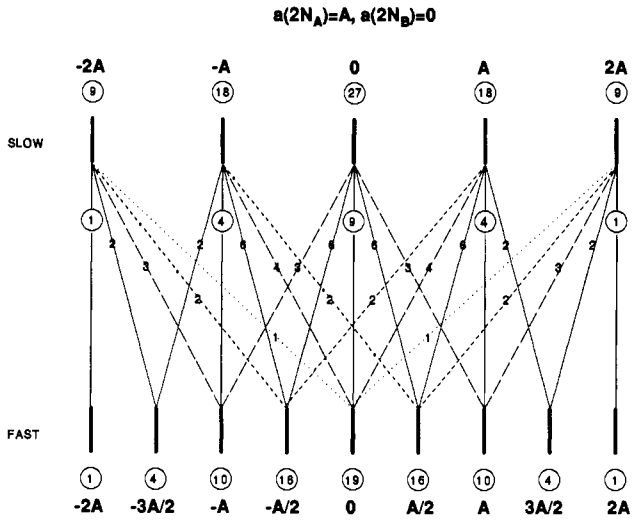

Figure 4. connecting slow and fast exchange spectra for a system exchanging pairs of nitrogens of splitting $a(2N) = A$ and $a(2N') = 0$.

Table II. Alternating Line Width Effect for $A(2N) = 11$ G, $A(2N') = 0$ Exchange

region	first derivative peak heights					$k_{ex}(s^{-1})$
	0	$\pm^1/_2A$	$\pm A$	$\pm^3/_2A$	$\pm 2A$	
fast limit	1	0.84	0.58	0.21	0.05	$>3 \times 10^8$
coalescence	1		0.44		0.11	6.8×10^7
slow limit	1		0.67		0.33	$<6 \times 10^7$

nitrogens with $a(2N) \sim 11$ G with one having $a(2N) = 0$ G. Stick spectra at slow and fast exchange for an idealized case with $a(2N) = A$ and $a(2N' = 0$ are illustrated in Figure 4. The five lines of the slow-exchange spectrum (top) appear at 0, $\pm A$, and $\pm 2A$ G from the center of the spectrum, with the degeneracies shown circled (relative intensities 3:2:1 reading from the center line out), while at fast exchange, the spectrum shows nine lines, with degeneracies for four equivalent nitrogens (intensities 19:16:10:4:1) and a line separation of $A/2$. At intermediate exchange rates, an alternating line width effect[19] will be observed because the components of the lines move as illustrated upon electron exchange. The intermediate lines (at $\pm nA/2$ in Figure 4) will be extremely broadened at the temperature of maximum broadening (the coalescence temperature), and only the components which do not move upon electron exchange (the 9:4:1 quintet shown circled) will remain unbroadened. The intensities of the outer lines relative to the center for this case are summarized in Table II. Although our spectra are mostly complicated by partially resolved hydrogen splittings and the nitrogen splittings are not identical but only close, k_{ex} is fast enough for $\mathbf{a7}^{\bullet+}$ (Figure 2) and for $\mathbf{s2}^{\bullet+}$ (Figure 3) to show fast-exchange-limit spectra, while it is slow enough for the bis(hydrazines) to show slow-exchange-limit spectra.

Russell and co-workers[20] pointed out that the coalescence spectrum will be observed when $k_{ex} = 6.22 \times 10^6(\Delta A, \text{G})$ or $6.8 \times 10^7 s^{-1}$ for $A = 11$ G and that above the coalescence temperature, where broadened intermediate lines are observed, if ΔW is the difference in peak-to-peak line width measured in the first-derivative ESR spectrum between the unbroadened outer line and the next intermediate, broadened line in gauss, $k_{ex} = 2.54 \times 10^6(\Delta A)^2/\Delta W$ or $3.07 \times 10^8/\Delta W$. The qualitative criteria for observation of fast- and slow-exchange spectra for our case are shown in Table II.

Optical Spectra of Radical Cation Oxidation States. The purplish solutions showing ESR spectra of hydrazine radical cations which are produced by oxidation of bis(hydrazines) **3** and **8** to their radical cations have maxima of broad absorption bands between 512 and 548 nm. The use of 1 equiv of silver nitrate as the oxidant produces significantly higher yields of the visible-absorbing radical cation than does the use of the far less soluble and more powerful oxidant nitrosonium hexafluorophosphate, as shown by the ϵ_{min} values calculated assuming a 100% yield of the absorbing species (Table III,$\mathbf{s3}^{\bullet+}$ entries). We suppose that use of NO^+ as oxidant results in extensive decomposition, possibly caused by formation of the dication. Figure 5 shows the spectrum of $\mathbf{a3}^{\bullet+}$. The monomeric hydrazine radical cation $\mathbf{14}^{\bullet+}$ has its optical maximum at 312 nm (ϵ 1700), and the presence of the visible band can only be reasonably attributed to the presence of the second, reduced hydrazine in the molecule. We assign these visible bands to Hush-type charge-transfer bands of the monocations and summarize the data in Table III. Extraction of the bandwidth from experimental spectra is frequently difficult because of band overlap problems, which we have for $\mathbf{A}^{\bullet+}$, where the CT band overlaps on the high-energy side with other, more intense absorptions. Values of the frequency where absorption has fallen to one-half that at the maximum on the low-energy side of the band ($\nu_{max} - \nu_{1/2,lo}$) are not obscured. It also appears from inspection of the high-energy side of the CT band that ($\nu_{1/2,hi} - \nu_{max}$) is slightly larger than ($\nu_{max} - \nu_{1/2,lo}$); observed CT band shape appears to be non-Gaussian, with larger width at the high-energy side of the band. Values of bandwidth estimated as twice ($\nu_{max} - \nu_{1/2,lo}$) and as ($\nu_{1/2,hi} - \nu_{1/2,lo}$) appear in Table III.

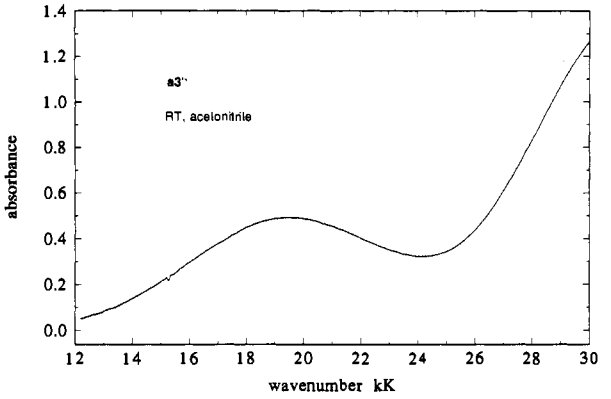

Figure 5. spectrum of $\mathbf{a3}^{\bullet+}$ in acetonitrile at room temperature.

As previously described,[6] electrolytic reduction of the monomeric diazenium salt $\mathbf{15}^{\bullet 0}$ produces hydrazyl radical $\mathbf{15}^{\bullet 0}$, which is stable in solution in the absence of oxygen.[6c] Reduction of the tetracyclic and hexacyclic bis(diazenium) salts $\mathbf{2}^{2+}$ and $\mathbf{7}^{2+}$ by either treatment with thiophenylate or electrolytic reduction produces blue-green solutions which contain the ESR signals of hydrazyl radicals and show absorptions in the near-IR region having two partially resolved maxima, a much broader band in the 1050–1200 nm-region, and an ill-resolved narrower second maximum on the long-wavelength (low-energy) side, as illustrated in Figure 6 for $\mathbf{s2}^{\bullet+}$ and $\mathbf{a7}^{\bullet+}$. There is likely to be an additional unresolved structure in each band, as indicated by the −25 °C spectrum in pyridine illustrated in Figure 7. The near-IR bands exhibit similar solvent and temperature dependence, although the narrower, low-energy band is only a shoulder in some solvents and has a higher absorption than the broader, higher energy band-(s) in others. The resence of these bands is attributed to Hush-type charge-transfer bands for the radical cations, and the data for $\mathbf{B}^{\bullet+}$ are summarized in Table IV. The low-energy band is clearly narrower than the higher energy envelope. Because both sets of bands move significantly when the solvent is changed, we believe they are all caused by CT absorption, and the total bandwidth at half-height of the near-IR region appears in the $W_{1/2}$ column of Table IV after the 1050–1200-nm band position and intensity information and is used in the discussion. See the

(19) Sullivan, P. D.; Bolton, J. R. *Adv. Magn. Reson.* **1970**, *4*, 39.
(20) Russell, G. A.; Underwood, G. R.; Lini, D. C. *J. Am. Chem. Soc.* **1969**, *89*, 6636.

Table III. Bis(hydrazine) Radical Cation Optical Data

compd	conditions[a]	$\lambda_m = E_{op}$ (nm ($\times 10^3$ cm^{-1}))	ϵ(min)[b] (M^{-1} cm^{-1})	$W_{1/2}$ ($\times 10^3$ cm^{-1})	ν_{12}(HTL) ($\times 10^3$ cm^{-1})	$W_{1/2}/\nu_{1/2}$HTL
s3$^{\bullet+}$	Ag, CH_3CN*	512 (19.5_3)	610	8.2,[c] 8.7[d]	6.70	1.22,[c] 1.30[d]
	NO, CH_3CN	520 (19.2_3)	(46)	7.7[c]	6.65	1.16[c]
	NO, CH_2Cl_2	556 (17.9_9)	(23)	6.9[c]	6.43	1.07[c]
	NO, $CHCl_3$	522 (19.1_6)	(–)	7.4[c]	6.70	1.10[c]
a3$^{\bullet+}$	Ag, CH_3CN*	514 (19.4_0)	560	8.8,[c] 9.7[d]	6.68	1.32,[c] 1.45[d]
	El, CH_3CN	520 (19.2_3)	590	8.6,[c] 9.9[d]		
a8$^{\bullet+}$	Ag, CH_3CN*	548 (18.2_5)	540	7.9,[c] 8.3[d]	6.48	1.22,[c] 1.18[d]

[a] Oxidant: Ag = $AgNO_3$ oxidation; NO = $NOPF_6$ oxidation; El = electrochemical oxidation (0.1 M tetrabutylammonium perchlorate as supporting electrolyte). An asterisk means Hush analysis of the data appears in Table VIII. [b] ϵ calculated assuming a 100% yield of radical cation. Numbers in parentheses for NO^+ oxidation obviously indicate low yield. [c] Bandwidth estimated as $2(\nu_{max} - \nu_{1/2,lo})$ (see text). [d] Bandwidth estimated from ($\nu_{1/2,hi} - \nu_{1/2,lo}$) (see text).

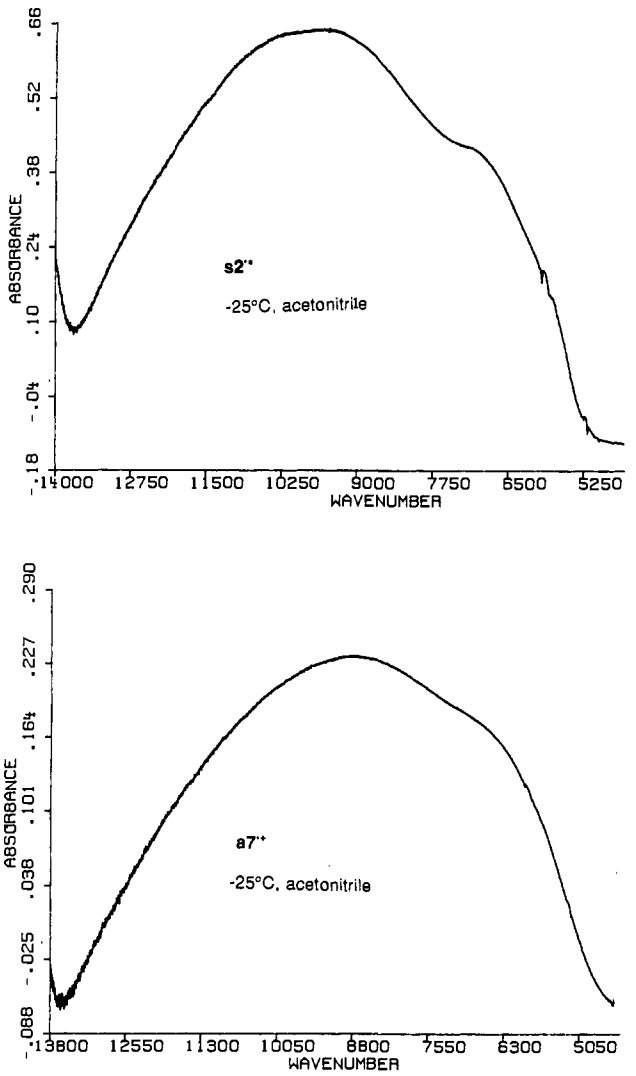

Figure 6. spectra of **s2**$^{\bullet+}$(top) and **a7**$^{\bullet+}$ (bottom) in acetonitrile at –25 °C.

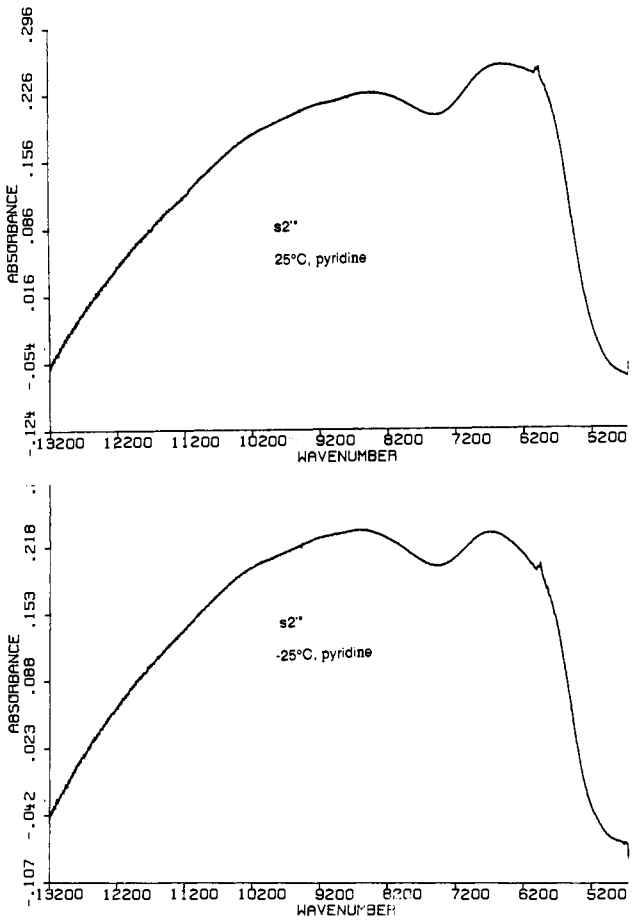

Figure 7. spectra of **s2**$^{\bullet+}$ in pyridine at +25 (top) and –25 °C (bottom).

supplementary material for additional details about the partially resolved longer wavelength bands.

The *inner* tetracyclic bis(diazenium) salt **13**$^{2+}$ also reduces to give a blue-green solution, but its near-IR spectrum is quite different from that of its *outer* bis(diazenium) analogues. A single absorption maximum at 850 nm, which is both more intense and narrower, is observed for **13**$^{\bullet+}$. We attribute this band to an electronic absorption and not a charge-transfer band. We were unable to find a band broad enough to attribute to a CT band in the near-IR or IR regions.

λ Values from Optical Spectra. Assuming that the bands reported in Tables III and IV are CT bands, $E_{op} = \lambda$ for intramolecular ET. E_{op} in acetonitrile at 25 °C is 52–56 kcal/mol for the four-σ-bond-linked **A**$^{\bullet+}$ examples and 24–27 kcal/mol for the corresponding **B**$^{\bullet+}$. The E_{op} values for the *anti* tetracyclic systems are larger than those for the hexacyclic ones, both for the hydrazine radical cations (tetracyclic **a3**$^{\bullet+}$, 55.5 kcal/mol; hexacyclic **a8**$^{\bullet+}$, 52.2 kcal/mol) and for the hydrazyl radical cations (tetracyclic **a2**$^{\bullet+}$, 26.4 kcal/mol; hexacyclic **a7**$^{\bullet+}$, 23.9 kcal/mol). This is reasonable if it is assumed that the tetracyclic systems have more twist at their CNNC units, which should raise E_{op} because twist at the CNNC bond in the oxidized dinitrogen vertical ET form is particularly costly in energy. The observed sensitivity of E_{op} to torsion of the polycyclic frameworks suggests to us that E_{op} is responding properly to a rather subtle structural change. E_{op} includes λ_{out} as well as λ_{in}, but λ_{out} ought to be very similar for **A**$^{\bullet+}$ and **B**$^{\bullet+}$ with the same connecting links, because the distances between the dinitrogen units are so similar. As expected because the λ_{out} values should be similar, the differences in E_{op} for **A**$^{\bullet+}$ and **B**$^{\bullet+}$ of the same systems are quite constant, 28.8 ± 0.5 kcal/mol (last column of Table V).

Table IV. Bis(hydrazyl) Radical Cation Optical Data

compd	conditions[a]	$\lambda_m = E_{op}$[b] (nm ($\times 10^3$ cm^{-1})	ϵ(min)[b,c] (M^{-1} cm^{-1})	$W_{1/2}$ ($\times 10^3$ cm^{-1})	$\nu_{1/2}$(HTL) ($\times 10^3$ cm^{-1})	$W_{1/2}/\nu_{1/2}$(HTL)
s2$^{\bullet+}$	PhS$^-$, CH_3CN	108^0 (9.26)	1110			
	El, CH_3CN[e] *	106_2 (9.42)	1450	6.50	4.65	1.40
	El, CH_3CN [–25 °C]	104_4 (9.58)	1550	6.54	4.69	1.39
	El,[f]	108_2 (9.24)	580	7.06	4.61	1.52
	El, DMSO	1027 (9.74)	965	7.46	4.73	1.58
	El, CH_2Cl_2	105_6 (9.47)	1200		4.67	
	El, CH_2Cl_2 [–25 °C]	104_9 (9.53)	1300			
	El, pyridine	118_9 (8.41)	1100	6.73	4.40	1.53
	El, pyridine [–25 °C]	116_5 (8.59)	1200	6.73	4.44	1.52
a2$^{\bullet+}$	PhS$^-$, CH_3CN	109_0 (9.17)				
	El, CH_3CN[a1] *	108_1 (9.25)	930	7.03	4.61	1.52
	El, CH_3CN[a2]	108_2 (9.24)	943	6.90		
a7$^{\bullet+}$	El, CH_3CN*	119^9 (8.34)	1350	6.80	4.38	1.55
	El, CH_3CN [–25 °C]	113_1 (8.84)	1400	6.28	4.51	1.39
	El,[f]	124_2 (8.05)	1255	6.67	4.30	1.55
	El,[f] [–25 °C]	117_1 (8.54)	1215	6.67	4.43	1.51
	El, DMF	112_6 (8.88)	1225	7.31	4.52	1.62
	El, DMF [–25 °C]	108_0 (9.26)	1225	7.56	4.61	1.64
	El, DMSO	106_9 (9.35)				
13$^{\bullet+}$	PhS$^-$, CH_3CN	850 (11.77)[g]	2300	4.08	5.20	0.78

[a] Reductant: PhS$^-$ (used as Me_4N^+ salt); El, electrolytic reduction using 0.1 M tetrabutylammonium perchlorate as supporting electrolyte, unless otherwise noted (a1, 0.04 M; a2, 0.4 M supporting electrolyte). Data recorded at room temperature (23–25 °C), except where noted at –25 °C in brackets. An asterisk means Hush analysis of the data appears in Table VIII. [b] For the broad, higher energy absorption envelope. See supplementary material for more information on the partially resolved, narrower, lower energy bands. [c] ϵ calculated assuming a 100% yield of radical cation. [d] Estimated using the entire width of the near-IR absorption at half-peak absorption. [e] Repetition of this experiment gave λ_m 1063 nm, ϵ 1450. [f] Solvent used is propylene carbonate. [g] Not attributed to a charge-transfer band (see text).

Table V. AM1 Calculations of λ_{in}' for Bis(hydrazine) and Bis(hydrazyl) Radical Cation and Comparison with E_{op}[a]

hydrazines					hydrazyls						
compd	λ_{in}[b]	J'[b]	E_{op}[c]	$(E_{op} - \lambda'_{in})$	compd	λ_{in}[b]	J'[b]	E_{op}[c]	$(E_{op} - \lambda'_{in})$	$\Delta\lambda'_{in}$[d]	ΔE_{op}[c,e]
					"Monomeric"						
14$^{0/\bullet+}$	46.5				**15**$^{\bullet 0/+}$	18.0					
					Tetracyclic						
s3$^{\bullet+}$	45.4		55.8	10.4	**s2**$^{\bullet+}$	18.5	(0.7)	26.9	8.4	26.9	28.9
a3$^{\bullet+}$	46.4	0.7	55.5	9.1	**a2**$^{\bullet+}$	17.1	1.1	26.4	9.3	29.3	29.1
					Hexacyclic						
s8$^{\bullet+}$	44.8	(1.2)			**s7**$^{\bullet+}$	17.3				27.5	
a8$^{\bullet+}$	45.0	1.4	52.2	7.2	**a7**$^{\bullet+}$	16.8	1.4	23.9	7.1	28.2	28.3

[a] Units: kcal/mol. [b] See text for definition of these quantities. [c] Using E_{op} values in CH_3CN at room temperature from Tables V and VI. [d] λ'_{in}[bis(hydrazine)$^{\bullet+}$] – λ'_{in}[bis(hydrazyl)$^{\bullet+}$]. [e] E_{op}[bis(hydrazine)$^{\bullet+}$] – E_{op}[bis(hydrazyl)$^{\bullet+}$].

The observed E_{op} values thus behave qualitatively as predicted in the Introduction, significantly larger values being observed for $\mathbf{A}^{\bullet+}$ than for $\mathbf{B}^{\bullet+}$. We shall now consider how well quantitative predictions of λ_{in} from semiempirical AM1 calculations, which we have argued work well for the closely structurally related sesquibicyclic hydrazines,[7] compare with the observed E_{op} values. The ground state for an intermolecular, neutral, radical cation self-ET reaction may be represented as [$\mathbf{n}^0$,$\mathbf{c}^+$], where **n** and **c** refer to the geometry-relaxed reduced and oxidized compounds, respectively, including both internal geometry and the solvent shell around them, and the superscripts represent the charges present. The vertical ET state is then [$\mathbf{n}^+$,$\mathbf{c}^0$], where neither internal geometry nor solvent shell had relaxed when charge was transferred, and the Marcus λ value is the free energy difference between them. The enthalpy contribution to λ_{in} is the difference in heats of formation for [$\mathbf{n}^+$,$\mathbf{c}^0$] and [$\mathbf{n}^0$,$\mathbf{c}^+$], which we call λ'_{in}.[7] λ'_{in} may be written as the sum of the relaxation energies of the cation radicals and neutral compounds (eq 7). The intramolecular ET of $\mathbf{A}^{\bullet+}$ uses this equation if charge is really localized on one dinitrogen unit, i.e., if the species is a candidate for a Hush theory analysis. For $\mathbf{B}^{\bullet+}$ the reduced species is a cation (relaxed form $\mathbf{c}^+$) and the oxidized one a dication (relaxed form $\mathbf{d}^{2+}$), so λ'_{in} uses eq 8.

$$\lambda'_{in}(\mathbf{A}^{\bullet+}) = \{\Delta H_f(\mathbf{n}^+) - \Delta H_f(\mathbf{c}^+)\} + \{\Delta H_f(\mathbf{c}^0) - \Delta H_f(\mathbf{n}^0)\} \quad (7)$$

$$\lambda'_{in}(\mathbf{B}^{\bullet+}) = \{\Delta H_f(\mathbf{c}^{2+}) - \Delta H_f(\mathbf{d}^{2+})\} + \{\Delta H_f(\mathbf{d}^+) - \Delta H_f(\mathbf{c}^+)\} \quad (8)$$

The results of AM1 calculations using geometry optimized structures and UHF energies for the open-shell radical cationic species are summarized in Table V. AM1 calculations get the charge to be strongly localized at one dinitrogen unit in the four -σ-bond-linked examples of both $\mathbf{A}^{\bullet+}$ and $\mathbf{B}^{\bullet+}$, as shown both by the geometries and λ'_n values calculated. The calculated differences in λ'_{in} (averaging 28.0 kcal/mol) are rather close to the observed differences in E_{op} for these systems (averaging 28.8 kcal/mol). The decrease in E_{op} for closing the tetracyclic compounds to hexacyclic ones is, however, significantly underestimated by $\Delta\lambda'_{in}$ of the AM1 calculations: ΔE_{op} for the *anti* hydrazines and hydrazyls are 2.7 and 2.5 kcal/mol, respectively, while the corresponding $\Delta\lambda'_{in}$ values are 0.6 and 0.3 kcal/mol, respectively. These errors are probably caused by the fact that AM1 calculations underestimate the amount of bicyclic torsion in 2,3-diazabicyclo[2.2.2]octane rings of hydrazines.[3,7,10b] Because AM1 calculations fail to predict enough torsion for tetracyclic systems, we suggest that the best comparisons to make in considering how well the calculated λ'_{in} values correlate with experimental λ_{in} values should be for the hexacyclic systems, for which E_{op}(CH_3CN, 25 °C) – λ'_{in} values are 7.2 and 7.1 kcal/mol for $\mathbf{a8}^{\bullet+}$ and $\mathbf{a7}^{\bullet+}$, repectively, and, if λ'_{in} were equal to λ_{in}, would be λ_{out} values (for CH_3CN at room temperature). As discussed below, these numbers appear to us to be close to λ_{out}.

Solvent effects on E_{op} have been important in the study of mixed-valence complexes. Plots of E_{op} versus the solvent parameter γ[21] (see eq 9) are linear for many mixed-valence

$$\gamma = (n_D^2)^{-1} - (\epsilon_s)^{-1} \quad (9)$$

complexes and often have been discussed using Marcus's simple λ_{out} evaluation (eq 10).[4] n_D is the refractive index at the sodium

$$\lambda_{out} = e^2 g(r,d)\gamma \quad (10)$$

D line, and $g(r,d)$ is a distance parameter, for which $[r^{-1} - d^{-1}]$ is often employed for mixed-valence complexes, with r the assumed radius of a "monomeric" center and d the metal–metal distance in the complex. Use of distances in angstroms with e^2 of 332.1 produces λ_{out} in kcal/mol. The general predictions of eq 10, seeing decrease in λ_{out} and hence in E_{op} with an increase in γ or a decrease in d, are certainly seen, but simple application of eq 10 appears insufficient to separate λ_{in} and λ_{out}. Two well-studied mixed-valence transition-metal complexes are **17**[22] and **18**,[23] which

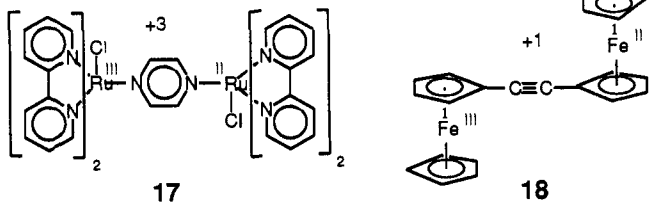

17

18

give linear E_{op} vs γ plots, but for which $\lambda_{out} \propto \gamma$ produces intercepts which are larger than is consistent with independent estimates of λ_{in} for the monomeric systems. Braunschweig and co-workers[24] discuss in detail the solvent sensitivity of E_{op} for ruthenium-centered complexes, including **17**. They point out that E_{op} is not simply $\lambda_{in} + \lambda_{out}$ for such complexes, because excited states are produced by irradiation into the CT band, and conclude that to a reasonable approximation, the spin–orbit coupling, λ_{so}, which is 1250 cm^{-1} (3.6 kcal/mol) for trivalent ruthenium, should also contribute to E_{op}. More complex ellipsoidal models for estimation of $g(r,d)$ are employed, and it is concluded that the observed E_{op} can indeed be reconciled with the estimated λ_{in} = 4.7 kcal/mol for the monomer using one of the $g(r,d)$ models and that the experimental slope is explained at least for ligands larger than the pyrazine of **17**; the decreased solvent dependence observed for a closely related system with the chlorides of **17** replaced by pyridine ligands remains unrationalized even with a larger bridging ligand.[24] Weaver and co-workers estimate λ_{in} for ferrocene (the "monomer" corresponding to **18**) at 2 kcal/mol (0.7×10^3 cm^{-1}),[25] and employ $E_{op}/4$ for **18** as an estimate of the solvent-dependent thermal barrier for self-ET of ferrocene.

Plots of E_{op} vs γ are not linear for our data, as shown in Figure 8. As indicated by the thermodynamic results, ion pairing becomes increasingly important in less polar solvents, and the increase in E_{op} observed for chloroform compared to methylene chloride for bis(hydrazine)$^{\bullet+}$ **s3**$^{\bullet+}$ may well have its origin here. The barrier for intermolecular self-ET for a sesquibicyclic hydrazine was

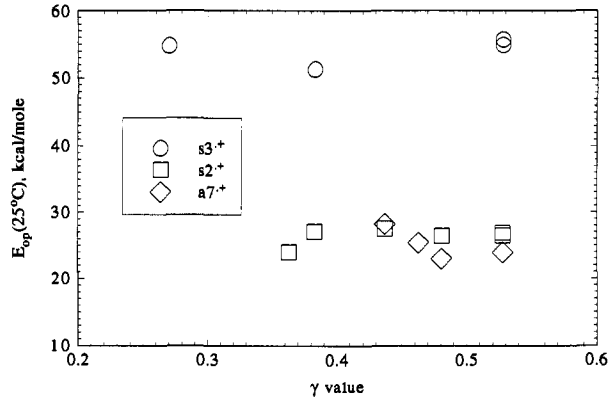

Figure 8. $_{op}$ vs γ plots for **s3**$^{\bullet+}$, **s2**$^{\bullet+}$, and **a7**$^{\bullet+}$ at 25 °C.

also observed to be "too high" in chloroform.[26] We have not properly tested the solvent dependence for **A**$^{\bullet+}$ because of lifetime problems. We hope to do this in the future, when we have prepared an isolable example which can be purified and dissolved in various solvents.

Although our **B**$^{\bullet+}$ data do not include very nonpolar solvents, the E_{op} vs γ plots of Figure 8 exhibit too much scatter to discern the negative slope predicted by eq 10. The near-IR region for **B**$^{\bullet+}$ probably consists of several overlapping components whose relative intensity may change with solvent; this is certainly true for the intensity of the partially resolved lower energy band relative to the higher energy envelope. Quantitative application of eq 10 to estimate λ_{out} for organic species is difficult. The atom positions for **B**$^{\bullet+}$ are rather well defined, but because charge is delocalized, neither r nor d is precisely known. For six bis-bicyclic hydrazines, the r values calculated from X-ray structures are $1.17_5 \pm 0.006$ times the r calculated from the volume occupied by the AM1 structure.[26a] Using r for **a2**$^{\bullet+}$ as 1.175 times the 3.26-Å AM1 radius of "monomer" **21**, i.e., 3.83 Å, and d as the 4.84-Å N–N′ distance (from Table III) gives $[r^{-1} - d^{-1}]$ of 0.0545 $Å^{-1}$, for which eq 10 predicts $\lambda_{out}(CH_3CN)$ of 9.6 kcal/mol. Analyses to be published separately for solvent effects on the self-ET rate constants for hydrazines[26b,c] are also consistent with a 10 kcal/mol $\lambda_{out}(CH_3CN)$ for the compounds studied here, and we shall employ this value for the calculations discussed below. As noted in Table V, the assumption that the AM1-calculated $\lambda_{in}' = \lambda_{in}$ produces $\lambda_{out}(CH_3CN)$ values of 7.1–10.4 kcal/mol for the compounds studied, which is in surprisingly good agreement with the above estimate.

***J* Values from Optical Spectra.** We shall next examine a Hush analysis of our 25 °C, acetonitrile data to see if our assignments of the visible bands of **A**$^{\bullet+}$ and all the near-IR bands of **B**$^{\bullet+}$ as CT bands are quantitatively reasonable. We employ eq 11 (eq

$$J, cm^{-1} = (2.06 \times 10^{-2}/d)(\epsilon \nu_{1/2} h\nu_{max})^{1/2} \quad (11)$$

25 in ref 5c) to estimate the electronic coupling matrix element J (which is half the separation of the ground-state and excited-state energy surfaces at the ET transition state). The values obtained (see Table VI) correspond to $J = 3.5 \pm 0.5$ kcal/mol for both **A**$^{\bullet+}$ and **B**$^{\bullet+}$. We expect similar values of J because the structures are so similar and believe that obtaining similar J values from such different-appearing bands in different optical regions is an encouraging indication that Hush's eq 11 works for these compounds. The J quoted is comparable to the 3.7 kcal/mol evaluated by Paddon-Row, Hush, and co-workers for the doubly

(21) Apparently introduced by Pekar, who employed it as an important parameter in the phonon theory of crystals: Pekar, S. I *Untersuchen über die Elektronen-theorie der Kristalle*, Akademie-Verlag: Berlin, 1954 (Russian edition, 1951).

(22) Powers, M. J.; Meyer, T. J. *J. Am. Chem. Soc.* **1980**, *102*, 1289.

(23) (a) Powers, M. J.; Meyer, T. J. *J. Am. Chem. Soc.* **1978**, *100*, 4393. (b) McManis, G. E.; Gochev, A.; Nielson, R. M.; Weaver, M. J. *J. Phys. Chem.* **1989**, *93*, 7733. (c) Blackbourn, R. L.; Hupp, J. T. *Ibid.* **1990**, *94*, 1788.

(24) Braunschwig, B. S.; Ehrenson, S.; Sutin, N. *J. Phys. Chem.* **1986**, *90*, 3659. For discussion of ion pairing effects, see especially ref 23c.

(25) McMannis, G. E.; Nielson, R. M.; Gokev, A.; Weaver, M. J. *J. Am. Chem. Soc.* **1989**, *111*, 5533.

(26) (a) Nelsen, S. F.; Wang, Y.; Powell, D. R.; Hayashi, R. K. *J. Am. Chem. Soc.* **1993**, *115*, 5246. (b) Nelsen, S. F.; Kim, Y.; Blackstock, S. C. *J. Am. Chem. Soc.* **1989**, *111*, 2045. (c) Nelsen, S. F.; Wang, Y., submitted for publication.

Table VI. Hush Analysis of Optical Data at 25 °C in Acetonitrile[a]

bis(hydrazine) radical cations						bis(hydrazyl) radical cations					
compd	J[b] (cm^{-1})	$h\nu_{in}$ (cm^{-1})	κ_{el}[c]	Γ_n[d]	k_{et}[e] (s^{-1})	compd	J[b] (cm^{-1})	$h\nu_{in}$ (cm^{-1})	κ_{el}[c]	Γ_n[d]	k_{et}[e] (s^{-1})
s3$^{\bullet+}$	1350	800	1.00	80	1.8×10^5	**s2**$^{\bullet+}$	1270	1400	1.00	24	9.4×10^9
	(3.9)	1000	1.00	380	6.0×10^5		(3.6)	1600	1.00	37	1.6×10^{10}
		1200	1.00	1600	3.0×10^6			1800	1.00	52	2.5×10^{10}
a3$^{\bullet+}$	1370	800	1.00	80	1.1×10^5	**a2**$^{\bullet+}$	1050	1400	1.00	14	5.7×10^9
	(3.9)	1000	1.00	370	6.7×10^5		(3.0)	1600	1.00	22	1.0×10^{10}
		1200	1.00	1500	3.4×10^6			1800	1.00	32	1.7×10^{10}
a8$^{\bullet+}$	1180	800	1.00	60	3.3×10^5	**a7**$^{\bullet+}$	1150	1400	1.00	14	1.8×10^{10}
	(3.4)	1000	1.00	240	1.7×10^6		(3.3)	1600	0.99	19	2.9×10^{10}
		1200	1.00	900	7.8×10^7			1800	0.99	25	4.5×10^{10}

[a] The data sets used are those marked with asterisks in Tables III and VI. The larger $W_{1/2}$ estimates were used for $\nu_{1/2}$ of the hydrazines. λ_{out} = 10.0 kcal/mol was employed.[26b] [b] Calculated using eq 11. Numbers in parentheses are J in kcal/mol. [c] Calculated using eqs 12a and 12b, ref 29. [d] Calculated using eq 13. [e] Calculated using eq 12.

four-σ-bond-linked dimethoxynaphthalene/dicyanoethylene radical anion **19**$^{\bullet-}$ by analysis of its CT band.[27a] It is larger than

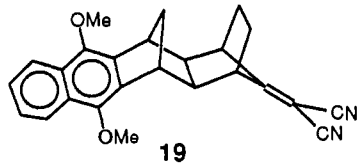

19

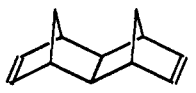

20

the J of 1.1 kcal/mol obtained for electronically excited neutral **19**,[27b] but it has been pointed out that larger J values are expected for a radical ion than a neutral compound.[27a] A larger J of 10.0 kcal/mol[5c] has been obtained in the gas phase by analysis of the PE spectum of doubly four-σ-bond-linked bis(alkene) **20**,[28] but the PE method, which deals with gas-phase, presumably delocalized radical cations, appears to consistently give larger J values than those for solvated, charge localized species. These doubly linked systems seem to be those most comparable to ours for which J has been estimated in the literature. We conclude that the J values obtained from eq 11 are consistent with our band assignments being correct and with Hush theory applying to these systems despite the anomalous band shape for **B**$^{\bullet+}$.

Estimation of Rate Constants for ET from the Optical Data. Table VI contains ET parameters and rate constants estimated from the optical data for hydrazines **s3**$^{\bullet+}$, **a3**$^{\bullet+}$, and **a8**$^{\bullet+}$ and hydrazyls **s2**$^{\bullet+}$, **a2**$^{\bullet+}$, and **a7**$^{\bullet+}$. We have employed eq 12, which

$$k_{et} = \kappa_{el}\nu_{in}(\lambda_{in}/\lambda)^{1/2}\Gamma_n \exp(-\lambda/4RT) \qquad (12)$$

includes the effects of nuclear tunneling, to estimate k_{et}, the rate constant for intramolecular electron exchange. The J values estimated from eq 11 are large enough to make the electron transmission coefficient κ_{el} of eq 12 be 1.0 for all entries of Table VI;[29] the ET is adiabatic. Equation 12 uses Holstein's nuclear tunneling transmission coefficient Γ_n, evaluated in eq 13 (which is eq 69 of ref 1a), and for brevity has been written employing $F = h\nu_{in}/4k_bT$.[30] The nuclear transition-state crossing (coupling)

$$\Gamma_n = \exp\{(-\lambda_{in}/h\nu_{in})(\tanh(F) - F)^{1/2}\} \qquad (13)$$

frequency, $h\nu_{in}$ (also called $\hbar\omega$ and $h\nu_q$ in various treatments[1,5]) has as usual been included by employing one effective value of $h\nu_{in}$ for a given system. Although the metal-centered systems of mixed-valence complexes have low $h\nu_{in}$ values (according to Hush, they probably do not much exceed 300 cm^{-1} for systems involving linked metal ions),[5c,d] organic compounds have much higher effective $h\nu_{in}$ values, which makes tunneling effects significant. For example, Grampp and Jaenicke[31] employ $h\nu_{in}$ of 1667 cm^{-1} for p-phenylenediamine self-ET, Closs, Miller, and co-workers[32] use 1500 cm^{-1} for mixed ET between aromatic radical anions and neutral aromatics in steroid-bridged systems, and Weaver, Nelsen, and co-workers[33] discussed possible values of 1500 and 1000 cm^{-1} for sesquibicyclic hydrazine self-ET. We include a range of $h\nu_{in}$ values in Table VI because the appropriate value to use is not clear. Larger $h\nu_{in}$ values are considered for **B**$^{\bullet+}$ than for **A**$^{\bullet+}$ because they should be larger for **B**$^{\bullet+}$; N=N stretches are significantly higher in frequency than N—N stretches, and the stretching frequency contribution to **B**$^{\bullet+}$ includes averages of (N=N)$^+$ and (N—N)$^\bullet$, while that for **A**$^{\bullet+}$ includes averages of (N—N)$^{\bullet+}$ and (N—N).

As shown in Table VI, **B**$^{\bullet+}$ examples are predicted from their optical spectra to show fast ET on the ESR time scale, as observed. For **A**$^{\bullet+}$, despite the very large λ value, the tunneling corrections are also large, and ET which is slow on the ESR time scale is predicted for rather small $h\nu_{in}$ values of $\leq$1200 cm^{-1}. AM1 calculations on sesquibicyclic hydrazines predict many low-frequency vibrations, and we obtained a prediction of $h\nu_{in}$ on the order of 1000 cm^{-1} for such compounds (using a summation weighted upon the change in pyramidality at nitrogen caused by the vibrations),[33] so we do not believe that such low $h\nu_{in}$ values are out of the question for **A**$^{\bullet+}$. The substantial agreement of the k_{et} values of Table VI with the limited information available from the ESR spectra of **A**$^{\bullet+}$ and **B**$^{\bullet+}$ suggests to us that our band assignments are correct and that Hush theory fits the optical spectra of these compounds rather well.

It will be noted from Table IV that lowering the temperature from +25 °C to −25 °C increases E_{op} 0.2–0.5 kcal/mol for **s2**$^{\bullet+}$

(27) (a) Penfield, K. W.; Miller, J. R.; Paddon-Row, J. W.; Cotsaris, E.; Oliver, A. M.; Hush, N. S. *J. Am. Chem. Soc.* **1987**, *109*, 5061. (b) Oevering, H.; Verhoeven, J. W.; Paddon-Row, M. N.; Warman, J. M. *Tetrahedron* **1989**, *45*, 4751.

(28) Paddon-Row, M. N.; Patney, H. K.; Brown, R. S.; Houk, K. N. *J. Am. Chem. Soc.* **1981**, *103*, 5575.

(29) κ_{el} is defined by eq 12a (eq 36 of ref 1a). The nuclear coupling frequency ν_{in}, s^{-1} = ch ν_{in}, cm^{-1},

$$\kappa_{el} = (1 - (\nu_{el}/2\nu_{in}))/(1 - 0.5(\nu_{el}/2\nu_{in})) \qquad (12a)$$

and ν_{el} is given by eq 12b (Table IV, case A of ref 1a),

$$\nu_{el} = (2J^2/h)(2\pi^3)^{1/2}/[2\lambda_{out}RT + (\lambda_{in}h\nu_{in})(\mathrm{csch}(h\nu_{in}/2k_bT)]^{1/2} \qquad (12b)$$

The result of ET being adiabatic for these systems does not depend upon our separation of λ_{out} and λ_{in}. Use of the simpler equation,[1] $\nu_{el} = g[J^2/(\lambda)^{1/2}]$, where $g = 2\pi/[\hbar(4RT)^{1/2}] = 1.51_7 \times 10^{14}$ (kcal/mol)$^{3/2}$ s^{-1} at 25 °C, gives $\kappa_{el} > 0.94$ for entries in Table VIII.

(30) We note that Hush[5c] employs a slightly larger nuclear tunneling transmission coefficient, Γ_n' of eq A: Γ_n'/Γ_n is 1.04 at $h\nu_{in}$ = 300 cm^{-1} and increases to 2.98 at $h\nu_{in}$ = 1800 cm^{-1}.

$$\Gamma_n' = [U\cosh(U)]^{-1/2}\,\Gamma_n, \quad \text{where } U = h\nu_{in}/2k_bT \qquad (A)$$

As discussed in the Bandwidth and Band Shape section, the bandwidths we observe do not support the use of the larger tunneling correction. Use of Hush's eq A would make the dotted $\Delta G^*(\omega)$ curves of Figure 9, **s2**$^{\bullet+}$ closer to the solid $\Delta G - J$ curve.

(31) (a) Grampp, G.; Jaenicke, W. *Ber. Bunsenges. Phys. Chem.* **1991**, *95*, 904. (b) γ(−25 °C)/ γ(25 °C) is 0.94 for propylene carbonate, 0.97 for acetonitrile, 0.98 for DMF, and 1.01 for methylene chloride.[29a]

(32) For a review, see: Closs, G. L.; Miller, J. R. *Science* **1988**, *240*, 440.

(33) Phelps, D. K.; Ramm, M. T.; Yang, Y.; Nelsen, S. F.; Weaver, M. J. *J. Phys. Chem.* **1993**, *97*, 181.

Table VII. Values of Hush's $g(\omega,T)$ (see eq 18)

$\hbar\omega$, cm^{-1}	g(−25 °C)	g(+25 °C)	g(−25 °C)/g(+25 °C)
300	1.114	1.081	1.031
600	1.360	1.272	1.069
900	1.624	1.493	1.088
1200	1.867	1.707	1.094
1500	2.086	1.904	1.096
1800	2.284	2.084	1.096

and 1.1–1.4 kcal/mol for $\mathbf{a7}^{\bullet+}$ in three solvents each. Using $\Delta G^* = E_{op}/4$, these changes correspond to small positive ΔS^* values (+0.9–2.6 and +5.4–7.2 cal/deg·mol, respectively). These results clear up what has been a semantic problem for us. Sutin[1a] and Grampp and Jaenicke[31] discuss tunneling effects in terms of a temperature-dependent inner-sphere barrier ($\lambda_{in}(T)$), and Grampp and Jaenicke use eqs 14 and 15 in their analyses of k_{ex}

$$\lambda_{in}(T) = Y\lambda_{in}^{\infty} \tag{14}$$

$$\text{where } Y = F^{-1}\tanh(F), \quad F = h\nu_{in}/4kT \tag{15}$$

measurements for (*p*-phenylenediamine)$^{0/\bullet+}$ intermolecular self-ET. However, if $E_{op} = \lambda$ decreased with temperature as λ_{in} does in eq 14, there would be large red shifts in $h\nu_{max}$ as the temperature was lowered. For example, if $\mathbf{B}^{\bullet+}$ had λ_{in}(25 °C) of 17.0 kcal/mol, λ_{in}(−25 °C) would decrease to 15.35–14.40 for $\hbar\omega$ of 900–1800 cm^{-1}, which corresponds to red shifts in $h\nu_{max}$ of 69–113 nm. λ_{out} is predicted to be proportional to γ, which also changes with temperature, but using Grampp and Jaenicke's compilation of γ values as a function of temperature,[31b] small to medium red shifts are predicted for three of the four solvents studied. The much smaller blue shift observed makes it clear that E_{op} measures $\lambda_t = \lambda_{out} + \lambda_{in}^{\infty}$, and not $\lambda_{in}(T)$. It seems misleading to state that λ_{in} decreases with temperature according to eq 14; it is not the energy separation for vertical electron transfer but the tunneling correction to the ET rate constant which eq 14 describes.

Bandwidth and Band Shape. We shall now consider the width of the CT bands observed here in somewhat more detail. Metal-centered mixed-valence complex CT bands have usually been identified[4] using Hush's criterion that the observed bandwidth (full width at half-height of the maximum absorption) is slightly greater than the high-temperature limit, $\nu_{1/2}$(HTL), shown in eq 16, where $h\nu_{max}$ is the CT band absorption maximum in cm^{-1} and

$$\nu_{1/2}(\text{HTL}),\ \text{cm}^{-1} = [(16\ln(2)k_bT)h\nu_{max}]^{1/2} \tag{16}$$

$[16\ln(2)k_hT]^{1/2}$ is 47.74 cm$^{1/2}$ at −25 °C and 47.94 at +25 °C. The high-temperature limit is only reached when $2k_bT$ (414 cm^{-1} at 25 °C) is much larger than $\hbar\omega$. The compounds studied here are clearly not at the high-temperature limit. In his 1985 review,[5c] Hush employs a larger expectation value of the bandwidth for systems having an appreciable $\hbar\omega$ value, recommending use of eqs 17 and 18 to estimate $\nu_{1/2}$:

$$\nu_{1/2} = g(\omega,T)\nu_{1/2}(\text{HTL}) \tag{17}$$

$$g(\omega,T) = [U\coth(U)]^{1/2}, \quad \text{where } U = h\nu_{in}/2k_bT \tag{18}$$

Values of $g(\omega,T)$ of interest here appear in Table VII. It will be noted that the ratios of observed bandwidth for the CT bands to $\nu_{1/2}$(HTL) are all greater than 1, but that they are less than $g(\omega,T)\nu_{1/2}$(HTL) using reasonable values for $h\nu_{in}$. It appears from our data that eq 17 overestimates $\nu_{1/2}$ at high $h\nu_{in}$ values for our compounds.[30] Another eq 17 prediction not confirmed by our experimental data for $\mathbf{s2}^{\bullet+}$ or $\mathbf{a7}^{\bullet+}$ is the 9% increase in $\nu_{1/2}$ predicted for $h\nu_{in} > 900$ cm^{-1} when the temperature is lowered from +25 °C to −25 °C. The $\mathbf{B}^{\bullet+}$ examples have slightly larger $W_{1/2}/\nu_{1/2}$(HTL) ratios than do $\mathbf{A}^{\bullet+}$ examples and obviously exhibit more complex band shapes; more than one band is starting to be resolved. We suggest that this beginning of resolution of structure occurs because of the high $h\nu_{in}$ values and low E_{op} values for $\mathbf{B}^{\bullet+}$.

Table VIII. Comparison of ET Parameters[a] for Mixed-Valence Organic Radical Cations with Organometallics

quantity	$\mathbf{s3}^{\bullet+}$	$\mathbf{s2}^{\bullet+}$	**17**	**18**
$E_{op} = \lambda$	19.5/55.8	9.4/26.9	7.7/22.0	7.5/21.4
λ_{in}	16.0/45.8[b]	5.9/16.9[b]	1.6/4.7[c]	0.7/2.0[d]
$\lambda_{out}(CH_3CN)$	3.5/10.0[b]	3.5/10.0[b]	4.8/13.7[e]	6.3/18.1[f]
J[g]	1.4/4.0	1.2/3.4	0.38–0.43[h]/ 1.1–1.2	030–0.38[i]/ 0.9–1.1
$h\nu_{1/2}$, cm^{-1}	est. 1000	est. 1500	≤300[k]	≤300[k]
$\Delta G^* - J/\Delta G^*$[m]	0.7	0.5	0.8[n]	0.8
$S = \lambda_{in}/h\nu_{in}$	∼16.5	∼3.9	>5.3	>2.3

[a] Units: × 10^3 cm^{-1} kcal/mol. [b] Obtainded using $E_{op} = \lambda_{in} + \lambda_{out}$, using λ_{out} = 10.0 kcal/mol (instead of the 7.5 kcal/mol used in Table VIII). [c] From ref 24. [e] Obtained using $E_{op} = \lambda_{in} + \lambda_{out} + \lambda_{so}$, using λ_{so} = 3.6 kcal/mol.[24] [f] Obtained using $E_{op} = \lambda_{in} + \lambda_{out} + \lambda_{so}$, using λ_{so} = 1.3 kcal/mol.[24] [g] Obtained using eq 11. [h] $\nu_{1/2}$ not reported;[22] these numbers use the 1.1–1.4 reported range of $\nu_{1/2}$(obs)/$\nu_{1/2}$(HTL). [i] $\epsilon(CH_3CN)$ not reported;[23a–c] we used an estimate of 300–500, from ϵ values in methylene chloride and nitrobenzene.[23a] The infinite dilution E_{op} and $\nu_{1/2}$ of 7.35 and 4.00 × 10^3 cm^{-1}, respectively,[21c] produce a J of 1.0 kcal/mol using ϵ of 500. [k] From ref 5c. [m] Using $\Delta G^* = E_{op}/4$. [n] Use of $\Delta G^* = (E_{op} - \lambda_{so})/4$ (see *e*) produces 0.7$_5$.

Conclusion

Use of Hush theory on the four-σ-bond-linked examples of $\mathbf{A}^{\bullet+}$ and $\mathbf{B}^{\bullet+}$ gives a set of E_{op} and J values which both appear reasonable on the basis of estimates from related compounds and which predict the qualitative ESR spectral result observed, that intramolecular ET is fast on the ESR time scale for $\mathbf{B}^{\bullet+}$ but slow for $\mathbf{A}^{\bullet+}$. We believe it is useful to compare the ET parameters derived for examples of $\mathbf{A}^{\bullet+}$ and $\mathbf{B}^{\bullet+}$ with literature data for the representative mixed-valence compounds, bis(ruthenium) bis(bipyridine) chloride **17** and bis(ferrocene) **18**; Table VIII makes this comparison at 25 °C in acetonitrile. The J values of for **17** and **18** were estimated using published data for metal–metal distance and optical spectra in acetonitrile,[22,23] employing eq 11. Figure 9 shows Marcus–Hush diagrams drawn to the same scale of the ET barrier regions of $\mathbf{s3}^{\bullet+}$, $\mathbf{s2}^{\bullet+}$, and **17** (**18** would look very similar) using data from Table VIII. The parabola crossover point is taken as $\Delta G^* = E_{op}/4$. The solid line representing the thermal barrier employs the relationship $\Delta G^*_{th} = \Delta G^* - J$. This classical relationship is made more complicated by nuclear tunneling effects. We have tried to represent tunneling effects by including curves for $\Delta G^*(\omega)$[34] for $\mathbf{s3}^{\bullet+}$ and $\mathbf{s2}^{\bullet+}$, obtained using eq 19, which employs eqs 14 and 15. These $\Delta G^*(\omega)$ curves

$$\Delta G^*(\omega) = (\lambda_{out} + Y\lambda_{in}^{\infty})/4 \tag{19}$$

are shown as dotted lines for $h\nu_{in}$ = 900 and 1200 cm^{-1} for $\mathbf{s3}^{\bullet+}$ (which lie slightly above and below the solid line shown for the ΔG^*_{th} curve). The ET barrier for $\mathbf{s2}^{\bullet+}$ is significantly broader, and the dotted $h\nu_{in}$ = 1500 and 1800 cm^{-1} curves shown both lie well above the ΔG^*_{th} curve. No $\Delta G^*(\omega)$ curve is shown for **17** because with its small estimated $h\nu_{in}$, its curve falls very close to the parabola crossover point; as often stated,[1,5] tunneling is not very important for metal-centered mixed-valence complexes. Table VIII and Figure 9 emphasize the special features of intramolecular ET in the organic compounds studied here. λ_{in} is larger for both organic compounds and is exceptionally large for $\mathbf{s3}^{\bullet+}$. These compounds have substantial J values relative to $\lambda/4$. The narrow barrier for $\mathbf{s3}^{\bullet+}$ causes large tunneling effects which would decrease the effective ΔG^*_{th} even further if the effective $\hbar\omega$ were large enough. Experimentally, ET is slow in the ESR time scale,

(34) Both Sutin[1a] and Grampp and Jaenicke[31] call this quantity $\Delta G^*(T)$, because they are concerned with temperature effects on tunneling.

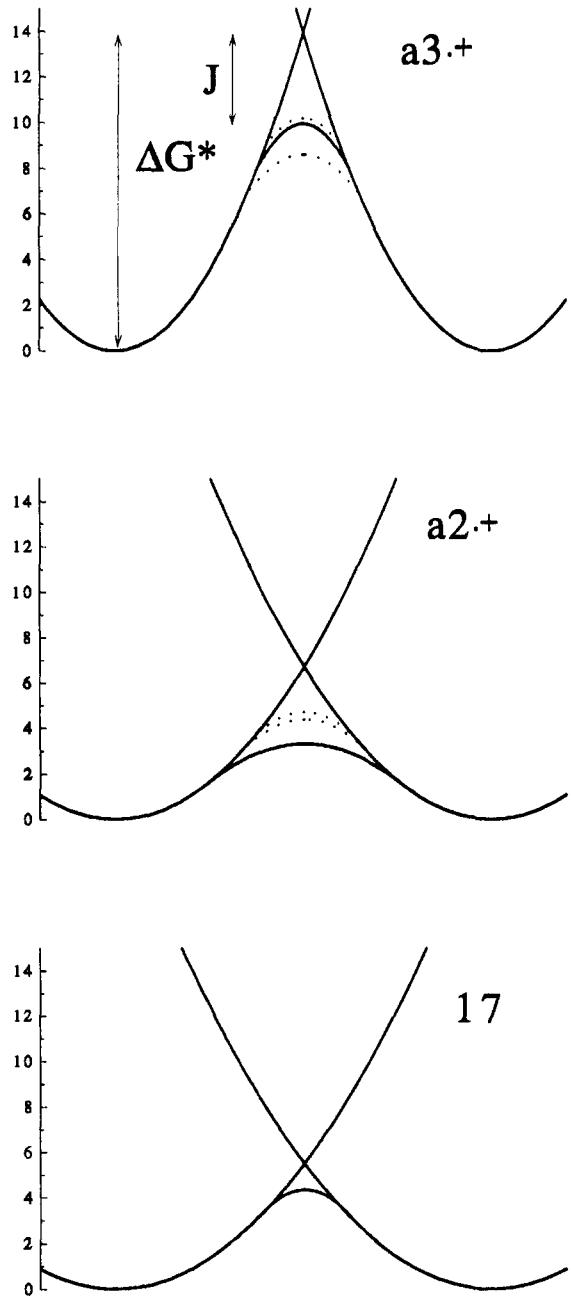

Figure 9. –Hush plots of the crossover region for examples of $A^{\cdot+}$ ($2^{\cdot+}$), $B^{\cdot+}$ ($3^{\cdot+}$), and a representative transition-metal mixed-valence compound (17) from data in Table VIII.

requiring that the effective $\hbar\omega$ of $A^{\cdot+}$ is rather low for an organic compound (*if* the oversimplified tunneling equation we used is indeed accurate, which can certainly be questioned). $s2^{\cdot+}$ has a ΔG^* more comparable to those of the transition-metal mixed-valence complexes, and although J is no larger than for that $s3^{\cdot+}$, it is so large relative to ΔG^* that use of eq 12 to calculate the rate constant appears to underestimate the rate constant compared to use of the classical approach of using $\Delta G^*_{th} = \Delta G^* - J$.[30]

Experimental Section

2,3,7,8-Tetrakis(ethoxycarbonyl)-2,3,7,8-tetraazahexacyclo-[7.4.1.0^{4,12}.0^{5,14}.0^{6,11}.0^{10,13}]tetradecane (5). A saturated solution of 2.0 g (4.2 mmol) of the diene **4**[1] in 1.3 L of dry acetone was placed in a 1.5-L photowell, deaerated with N_2 for 1 h, and photolyzed for 5 h with a 450-W Hanovia mercury lamp fitted with a Vycor filter. Solvent was removed by evaporation. A second batch of 1.2 g (2.5 mmol) of the diene was treated similarly. The combined photolysis products were vacuum distilled (80 °C; 0.1 mmHg) to remove the low-boiling, acetone-derived side products. The remaining mixture crystallized to form a yellow solid, which was in turn recrystallized from hot methanol. The remaining yellow oil was purified by flash chromatography on 40–60 μm of silica gel, using 50:50 ethyl acetate:methylene chloride, and the resulting yellow oil was recrystallized from ether at –20 °C, giving **5** (2.79 g, 5.8 mmol, 87%, lit.[9] 90%), mp 153–154 °C (lit.[9] mp 155–156 °C): ^{1}H NMR (200 MHz, $CDCl_3$) δ 4.23 (12 H, m), 3.20–2.90 (6 H, m), 1.28 (12 H, m).

2,3,7,8-Tetraazahexacyclo[7.4.1.0^{4,12}.0^{5,14}.0^{6,11}.0^{10,13}]tetradeca-2,7-diene (6). In a 50-mL 3-necked round-bottomed flask fitted with a condenser and a gas inlet adapter, a mixture of 640 mg (1.34 mmol) of the tetraester **5**, 2.0 g (30.30 mmol) of powdered 85% KOH pellets, and 25 mL of dry, degassed methanol was refluxed under nitrogen for 1.5 h. After cooling, this mixture was poured into a beaker containing 4 mL of concentrated HCl, 40 g of ice, and 40 g of distilled water with stirring. This solution was warmed to 40 °C, removed from heat, and neutralized to pH 7 with 5 N NH_4OH solution. A 1.4-mL portion of 2 N $CuCl_2$ solution was added dropwise with occasional stirring. The red-brown precipitate was collected on a Buchner funnel; neutralization and precipitation were repeated twice. The copper salt was washed with NH_4Cl, 95% ethanol, and cold distilled water and then air-dried for 3 h, giving 600 mg of the copper complex of **6**. To a vigorously stirred slurry of 600 mg of the copper complex in 10 mL of distilled water was added dropwise an ice-cooled solution of 400 mg (10.0 mmol) of NaOH in 10 mL of distilled water. The resulting yellow-green mixture was extracted 4 times with 15-mL portions of methylene chloride. The grass-green aqueous layer was stirred overnight with 50 mL of methylene chloride. The combined organic layers were dried over $MgSO_4$, filtered, and evaporated. The crude product was purified by sublimation (0.16 mmHg) using an oil bath at 120 °C to give **6**, (89.8 mg, 0.482 mm, 36%), mp > 280 °C (lit.[9] mp 320 °C, sealed tube): ^{1}H NMR (200 MHz, $CDCl_3$) δ 5.63 (s, 4H), 2.44 (s, 4H), 1.73 (s, 2H).

2,8-Bis(dimethylethyl)-2,8-diazonia-3,7-diazahexacyclo-[7.4.1.0^{4,12}.0^{5,14}.0^{6,11}.0^{10,13}]tetradeca-2,7-diene Bis(tetrafluoroborate) ($s7^{2+}(BF_4^-)_2$ and 2,7-Bis(dimethylethyl)-2,7-diazonia-3,8-diazahexacyclo-[7.4.1.0^{4,12}.0^{5,14}.0^{6,11}.0^{10,13}]tetradeca-2,7-diene Bis(tetrafluoroborate) ($a7^{2+}(BF_4^-)_2$. In an oven-dried 25-mL round-bottomed flask with a stirbar and a rubber septum, a mixture of 100 mg (0.537 mmol) of bis(azo) compound **6** and 10 mL of *tert*-butyl alcohol was degassed with a nitrogen stream, and 0.18 mL (2 equiv, 1.07 mmol) of $HBF_4{\cdot}OEt_2$ was added. The mixture was refluxed 20 h, cooled, and stirred with 20 mL of ether. The solvents were decanted and the solid collected, and evaporation of the solvent gave a total of 230 mg of yellow solid. Two recrystallizations from CH_3CN/ether at –20 °C gave 76 mg (0.16 mmol, 30%) of large, white, squarish crystals shown by ^{13}C NMR showed to be exclusively the *anti* isomer, mp 199–202 °C dec. $a7^{2+}$: ^{1}H NMR (200 MHz, CD_3CN) δ 6.45 (br s, 2 H), 6.19 (br s, 2H), 3.03 (br s, 4 H), 2.61 (br s, 2H), 1.71 (2, 18 H); ^{13}C NMR (67.5 MHz, CD_3CN) δ 83.08 (C), 70.93 (CH), 65.68 (CH), 44.60 (CH), 42.42 (CH), 41.44 (CH), 26.47 (CH_3). Anal. Calcd for $C_{18}H_{28}B_2F_8N_4$: C, 45.59; H, 5.96; N, 11.82. Found: C, 45.45; H, 5.83; N, 11.73.

The mother liquors were concentrated and dissolved in hot methanol. Cooling to –20 °C resulted in slightly orange spherical clusters of needle-like crystals (80 mg, mmol, 31%), mp 190–200 °C. A second recrystallization from CH_3CN/MeOH resulted in 30 mg of white crystals but did not improve the ratio of isomers, shown by NMR to be ~15% *anti*, 85% *syn*. $s7^{2+}$: ^{1}H NMR (200 MHz, CD_3CN) δ 6.50 (m, 2 H), 6.16 (m, 2 H), 3.02 (m, 4 H), 2.59 (m, 2 H), 1.70 (s, 18 H); ^{13}C NMR (125 MHz, CD_3CN) δ 82.93 (C), 71.29 (CH), 65.07 (CH), 44.95 (CH), 44.03 (CH), 41.84 (CH), 41.77 (CH), 26.38 (CH_3).

2,7-Bis(dimethylethyl)-3,8-dimethyl-2,3,7,8-tetraazahexacyclo-[7.4.1.0^{4,12}.0^{5,14}.0^{6,11}.0^{10,13}]tetradecane (a8). In an oven-dried 25-mL round-bottomed flask with a stirbar and a rubber septum, a mixture of 76 mg (0.16 mmol) of $a7^{2+}$ and 2 mL of THF was degassed with a stream of nitrogen. A 0.69-mL (6 equiv, 0.97 mmol) portion of 1.4 M MeLi solution was added slowly by syringe. The mixture cleared in 5 min to give a colorless solution. The reaction was stirred for 1.5 h and then quenched with 2 mL of saturated NH_4Cl solution. Extraction with ether (3 × 30 mL), followed by drying over Na_2SO_4 and evaporation, gave a white solid. The product **a8** was crystallized twice from acetone/hexane at –20 °C, (93.7%) mp 107–108 °C: MS calcd for $C_{20}H_{34}N_4$, 330.2776, found 330.2802; ^{1}H NMR (500 MHz, CD_3CN) δ 2.95–3.03 (complex, 4H), 2.67–2.86 (complex, 6H), {2.57 (**A** + **C**), 2.38 (**B**), 2.39 (**C**), 3 s, 6H, NCH_3}, {1.078 (**A**), 1.16 (**B**), 1.09 (**C**), 1.081 (**C**), 4 s, 18 H, CCH_3}; mole fractions from intetration of the NCH_3 region, **A**, 0.56_8, **B**, 0.28_8, **C**, 0.14_4, and of the CCH_3 region, **A**, 0.56_3, **B**, 0.28_8, **C**, 0.14_8; ^{13}C NMR (125 MHz, $CDCl_3$) δ, **A**, 28.32(CH_3), 33.06 (CH), 33.17 (CH), 37.38

(CH), 49.65 (CH_3), 50.42 (CH), 58.24 (CH), 58.25 (C_q), B, 28.28 (CH_3), 29.70 (CH), 34.31 (CH), 37.57 (CH), 48.02 (CH_3), 52.24 (CH), 57.76 (CH), 58.36 (C_q), C, 28.55, 28.60, (the smaller intensity minor conformation peaks have not been reliably located).

Bis(adduct) of MTAD with 1,6-Methano[10]annulene (10).[35] A solution of 158 mg (1.40 mmol) of 4-methyl-1,2,4-triazoline-3,5-dione (MTAD) in 10 mL of methylene chloride was added to a solution of 101 mg (0.70 mmol) of 1,6-methano[10]annulene (**9**)[12] in 10 mL of methylene chloride and allowed to stand for 2.5 h at room temperature, and a few drops of annulene solution was added to decolorize the residual MTAD. Evaporation of solvent followed by drying in vacuo gave 260 mg (0.706 mmol) of **10**, mp 136–142 °C dec (lit.[35] mp 253–254 °C): ^{1}H NMR (200 MHz, $CDCl_3$) δ 6.17 (4H, t, J = 3.6 Hz), 5.38 (4H, t, J = 3.6 Hz), 2.97 (6H, s), 0.97 (2H, s).

Hydrogenation of 10 to 11.[13] A solution of 2.40 g (6.51 mmol) of bis(adduct) **10** in 70 m of hot glacial acetic acid (distilled) in a glass autoclave liner was treated with 1 g of 10 % Pd/C catalyst (Aldrich), and with the aid of a booster pump, hydrogen pressure was taken to 4800 psi, the temperature was raised to 80 °C, and both were maintained for 50 h with shaking of the reaction chamber. After the autoclave was cooled and dismantled, the reaction mixture was filtered over Celite and washed with hot glacial acetic acid. The solvent was removed by evaporation to give a reddish-brown solid which was chromatographed on silica gel (10% MeOH, $CHCl_3$). The 2.0 g of product was determined to contain 60% (1.20 g) of **11** and 40% (0.80 g) of starting material **10**: yield 49% (lit.[13] yield 77%); mp > 280 °C (lit.[13] mp > 340 °C); ^{1}H NMR (200 MHz, $CDCl_3$/ methanol-d_4) δ 4.46 (m, 2H), 4.29 (m, 2H), 2.99 (s, 6H), 2.45–1.75 (m, 9H), 1.38 (s, 3H).

2-Methyl-11,12,13,14-tetraazatetracyclo[6.2.2.2^{3,6}.0^{2,7}]tetradeca-11,-13-diene (12). A mixture of 2.00 g (4.35 mmol) of **10**, 180 mL of 2-propanol, and 2.6 g (39.4 mmol) of KOH pellets (85%) was refluxed under nitrogen for 40 h. The reaction was cooled to room temperature, acidified to pH 2 with 2 N HCl, and treated with 25 g (0.18 mol) of $CuCl_2$ in 600 mL of distilled water. After the mixture was stirred at room temperature for 2 h, a 30-mL portion of concentrated NH_4OH was added to give a blue solution which was extracted with methylene chloride (4 × 100 mL). The combined organic layers were washed with distilled water (2 × 10 mL), dried over $MgSO_4$, filtered, and evaporated. The product was purified by column chromatography on silica gel (5% MeOH/ $CHCl_3$), followed by slow crystallization from CH_2Cl_2. A total of 627 mg (71%, lit.[11] 80%) of **12** was collected as light yellow crystals, mp 220–222 °C (lit.[11] mp 231 °C: ^{1}H NMR (200 MHz, $CDCl_3$) δ 5.11 (d, 4.5 Hz, 2H), 4.81 (t, 2.6 Hz, 2H), 2.00–1.80 (m, 2H), 1.60–1.40 (m, 3H), 1.40–1.20 (m, 2H), 1.19 (s, 3H), 0.85 (m, 2H).

2-Methyl-11,14-bis(dimethylethyl)-11,14-diazonia-12,13-diazatetracyclo-[6.2.2.2^{3,6}.0^{2,7}]tetradeca-11,13-diene Bis(tetrafluoroborate) ($13^{2+}(BF_4^-)_2$). A mixture of 82 mg (0.40 mmol) of bis(azo) compound **12**, 20 mLof *t*-BuOH, and 0.133 mL (2 equiv, 0.80 mmol) of HBF_4·OEt_2 was prepared under nitrogen in an oven-dried 50-mL round-bottomed flask with a rubber septum and refluxed for 48 h. Filtration gave an orange solid which proved to be the monobutylated product. This material was subjected to an additional 0.100 mL of acid and 10 mL of *t*-BuOH and refluxed for 30 h more. Addition of acid and alcohol was repeated until the reaction was complete. Concentration of the solution and addition of acetone gave slightly orange crystals which were recrystallized from CH_3CN and ether to give $13^{2+}(BF_4^-)_2$, mp 196–200 °C dec, 152 mg (0.309 mmol, 77%). Only one diastereomer was seen by NMR, and the *anti* relation of the *t*-butyl groups was assigned on the basis of the asymmetry of the NMR spectra: ^{1}H NMR (500 MHz, CD_3CN) δ 6.11 (m, 1H), 6.00 (m, 1H), 5.93 (m, 1H), 5.78 (m, 1H), 3.05 (m, 2H), 2.65–2.75 (m, 1H), 2.55–2.63 (m, 1H), 2.25–2.35 (m, 2H), 1.76 (s, 9H), 1.70 (s, 9H), 1.63 (s, 3H), 1.50–1.65 (m, 1H), 1.35–1.45 (m, 1H), 1.05–1.15 (m, 1H); ^{13}C NMR (125 MHz, CD_3CN) δ 85.15 (C), 84.27 (C), 76.99 (CH), 73.21 (CH), 71.65 (CH), 68.15 (CH), 46.17 (CH), 42.09 (CH), 26.58 (CH_3), 26.07 (CH_3), 25.25 (CH_2), 25.22 (CH_2), 24.55 (CH_2), 23.75 (CH_2), 21.90 (CH_3). Anal. Calcd for $C_{19}H_{34}B_2F_8$: C, 46.36; H, 6.98; N, 11.385. Found: C, 46.27; H, 6.91; N, 11.33.

Instrumentation. NMR spectra were taken on Bruker WP-200, WP-270, or AM-500 spectrometers. ESR spectra were taken on a Bruker ESP 300E spectrometer. UV/visible spectra were taken on a Hewlett-Packard 8452A diode array spectrophotometer, using matched 1-cm quartz cells. Near-IR spectra were taken on (a) a Nicolet 740 spectrophotometer, using a Pb–Se detector, with a 1 mm quartz-window cell, and a Specac apparatus for low-temperature work, or (b) a Cary 17-D spectrophotometer using matched 1-cm quartz cells.

Electrochemistry. Cyclic voltammograms were run at 2 mM, using as supporting electrolyte 0.1 M tetrabutylammonium perchlorate (Kodak or Fluka, recrystalized from hot 1:1 ethanol:water and dried at 110 °C before use). An EG&E PAR Model 273 instrument interfaced to an IBM PC-XT was employed. A Corning ceramic junction SCE was employed as reference electrode. Either a gold or a platinum disc working electrode was used, and the disc was polished at least between every two scans when hydrazines were studied. Coulometry used a modified CV cell, with a Pt foil working electrode fused to the bottom of the cell and a Pt wire counter electrode in a side arm separated from the main compartment by a glass frit. The solution was stirred with a stream of nitrogen introduced through a Teflon-brand (duPont) needle. Electrolysis was carried out by applying a constant potential 0.2 V past the oxidation/ reduction potential of the compound until the current dropped to the predetermined background level.

Calculations. AM1 calculations[36] used the VAMP program (version 4.4)[37] modified for use on a Stardent 3000 computer. Saunders's MM2[10a] structure search program VAXMOL5[38] was modified by Peter A. Petillo to allow use of a VAX 8650 to input structures generated from molecular orbital calculations, using program NEWSEL, written by P.A.P.

Acknowledgment. We thank the National Institutes of Health for partial financial support of this work under grant GM 29541, the Humboldt Foundation for a Lynen grant to J. J. W., and the National Science Foundation for an International Cooperative Research supplement for J. A. Preliminary work in this area by Mary K. Van Atten (M.S., University of Wisconsin, 1989) is gratefully acknowledged. We are indebted to Dr. H. Reis (BASF, Ludwigshaven) for providing the cyclooctatetraene used in this work, to Prof. H. Prinzbach (University of Freiburg) for unpublished experimental details for the preparation of **10-12**, to Prof. W. Grimme (University of Köln) for unpublished experimental details for the preparation of basketene, to Dr. T. Clark (University of Erlangen-Nürnberg) for his VAMP programs, to Prof. M. Saunders for his stochastic structure search molecular mechanics program, and to Prof. D. H. Evans for software for simulation of CV curves.

Supplementary Material Available: Cyclic voltammetry data and discussion for **A** in CH_2Cl_2 and **B** in DMSO; tabulation of λ_m, ϵ_{min}, and estimated $W_{1/2}$ values for the $\mathbf{B}^{\bullet+}$ entries of Table IV (7 pages). This material is contained in many libraries on microfiche, immediately follows this article in the microfilm version of the journal, and can be ordered from the ACS; see any current masthead page for ordering information.

(35) Askenazi, P.; Ginsburg, D.; Vogel, E. *Tetrahedron* **1977**, *33*, 1169.

(36) Dewar, M. J. S.; Zoebisch, E. G.; Healey, E. F.; Stewart, J. J. P. *J. Am. Chem. Soc.* **1985**, *107*, 3902.

(37) Clark, T.; Rauhut, G., unpublished.

(38) Saunders, M. *J. Am. Chem. Soc.* **1987**, *109*, 3150.